Journal of Visualized Experiments

Whole Ovary Immunofluorescence, Clearing, and Multiphoton Microscopy for Quantitative 3D Analysis of the Developing Ovarian Reserve in Mouse

--Manuscript Draft--

Article Type:	Invited Methods Collection - JoVE Produced Video
Manuscript Number:	JoVE62972R2
Full Title:	Whole Ovary Immunofluorescence, Clearing, and Multiphoton Microscopy for Quantitative 3D Analysis of the Developing Ovarian Reserve in Mouse
Corresponding Author:	Ewelina Bolcun-Filas Jackson Laboratory Bar Harbor, Maine UNITED STATES
Corresponding Author's Institution:	Jackson Laboratory
Corresponding Author E-Mail:	Ewelina.Bolcun-filas@jax.org
Order of Authors:	Ruby Boateng
	Nathaniel Boechat
	Philipp Henrich
	Ewelina Bolcun-Filas
Additional Information:	
Question	**Response**
Please specify the section of the submitted manuscript.	Developmental Biology
Please indicate whether this article will be Standard Access or Open Access.	Standard Access ($1400)
Please indicate the **city, state/province, and country** where this article will be **filmed**. Please do not use abbreviations.	Bar Harbor, Maine, US
Please confirm that you have read and agree to the terms and conditions of the author license agreement that applies below:	I agree to the Author License Agreement
Please provide any comments to the journal here.	
Please confirm that you have read and agree to the terms and conditions of the video release that applies below:	I agree to the Video Release

TITLE:

Whole Ovary Immunofluorescence, Clearing, and Multiphoton Microscopy for Quantitative 3D Analysis of the Developing Ovarian Reserve in Mouse

Ruby Boateng, Nathaniel Boechat, Philipp P. Henrich[#], Ewelina Bolcun-Filas

The Jackson Laboratory, Bar Harbor, ME 04609, USA

Microscopy Service at The Jackson Laboratory

Email addresses of co-authors:

Ruby Boateng (Ruby.Boateng@jax.org)
Nathaniel Boechat (Nathaniel.Boechat@jax.org)
Philipp P. Henrich (Philipp.Henrich@jax.org)

Corresponding author:

Ewelina Bolcun-Filas (Ewelina.Bolcun-filas@jax.org)

SUMMARY:

Here, we present an optimized protocol for imaging entire ovaries for quantitative and qualitative analyses using whole-mount immunostaining, multiphoton microscopy, and 3D visualization and analysis. This protocol accommodates high-throughput, reliable, and repeatable processing that is applicable for toxicology, clinical diagnostics, and genomic assays of ovarian function.

ABSTRACT:

Female fertility and reproductive lifespan depend on the quality and quantity of the ovarian oocyte reserve. An estimated 80% of female germ cells entering meiotic prophase I are eliminated during Fetal Oocyte Attrition (FOA) and the first week of postnatal life. Three major mechanisms regulate the number of oocytes that survive during development and establish the ovarian reserve in females entering puberty. In the first wave of oocyte loss, 30–50% of the oocytes are eliminated during early FOA, a phenomenon that is attributed to high long interspersed nuclear element-1 (LINE-1) expression. The second wave of oocyte loss is the elimination of oocytes with meiotic defects by a meiotic quality checkpoint. The third wave of oocyte loss occurs perinatally during primordial follicle formation when some oocytes fail to form follicles. It remains unclear what regulates each of these three waves of oocyte loss and how they shape the ovarian reserve in either mice or humans.

Immunofluorescence and 3D visualization have opened a new avenue to image and analyze oocyte development in the context of the whole ovary rather than in less informative 2D sections. This article provides a comprehensive protocol for whole ovary immunostaining and optical clearing, yielding preparations for imaging using multiphoton microscopy and 3D modeling using commercially available software. It shows how this method can be used to show the dynamics of oocyte attrition during ovarian development in C57BL/6J mice and quantify oocyte loss during the three waves of oocyte elimination. This protocol can be applied to prenatal and early

postnatal ovaries for oocyte visualization and quantification, as well as other quantitative approaches. Importantly, the protocol was strategically developed to accommodate high-throughput, reliable, and repeatable processing that can meet the needs in toxicology, clinical diagnostics, and genomic assays of ovarian function.

INTRODUCTION:

Most mammalian females are born with a finite number of meiotically arrested oocytes stored within primordial follicles, constituting the ovarian reserve (OR)[1,2]. The OR determines the overall female reproductive lifespan and health[3]. The OR normally declines in size with aging and can be prematurely depleted upon exposure to certain genotoxic agents (radiation/chemotherapy) and environmental stresses (malnutrition), leading to infertility[4–6]. Idiopathic female infertility can often be attributed to the genetic and physiological quality of eggs developing from the OR and remains poorly understood[7,8]. Because female follicle endowment is largely predetermined by birth, it is essential to understand the regulatory mechanisms involved in the OR establishment and maintenance.

In mice, OR formation starts with the specification of primordial germ cells (PGCs) around Embryonic day (E) 7.5[2]. The PGCs migrate to the genital ridges, where they will reside by approximately E10.5[9]. The following extensive proliferation occurs with incomplete cytokinesis resulting in the formation of cysts that will be broken down later in development[10,11]. At approximately E12.5, gonadal sex is determined, and PGC proliferation halts in ovaries. In females, PGCs, now oocytes, enter meiotic prophase I (MPI) at approximately E13.5[12,13]. Oocytes progress through extended MPI and arrest at the dictyate stage around the time of birth. During the first week after birth, each arrested oocyte is surrounded by granulosa cells, thereby forming a primordial follicle.

The number of primordial follicles in the OR of a female depends on how many oocytes survived the waves of oocyte elimination that occur before and during MPI arrest through apoptosis, autophagy, or necrosis[14,15]. The first wave occurs during fetal development and is known as FOA. FOA is an evolutionarily conserved process in females (mammalian and non-mammalian), whereby an estimated 50–80% of the oocytes are eliminated depending on the female species[16–19]. In mice, FOA occurs during E15.5 to E18.5 and has been attributed to the reactivation and expression of retrotransposon LINE-1 sequences causing oocyte death[20,21]. The second wave of oocyte elimination occurs through a meiotic checkpoint that eliminates oocytes with meiotic defects such as unrepaired DNA double-strand breaks (DSBs)[22,23]. The next wave of oocyte elimination occurs during cyst breakdown, culminating during the formation of primordial follicles, each of which contains a single oocyte[10,11,24,25].

In mice, the primordial follicle reserve is largely established by puberty, after which it decreases as primordial follicles are activated for growth during regular reproductive cycles. The OR size varies among individual women and among different genetic strains of mice; yet, the genetic regulation of OR size is not well understood[26–29]. Genetic studies of OR regulation are hampered by the lack of standardized protocols to study the waves of oocyte elimination during prenatal and postnatal development. Several oocyte quantification methodologies have been developed

in mice, with the most common and widely used being histomorphometric evaluation of histological sections[30,31]. In this technique, oocytes are identified on serial sections with histological stains, such as hematoxylin and eosin (H&E) and periodic acid–Schiff (PAS) or fluorescent markers. This technique is reliable if all conditions remain constant, including section thickness, efficient recovery of all sections throughout the ovary, and the counting schemes of individual laboratories. However, numbers reported by different laboratories often differ significantly and thus are not easily comparable.

Moreover, given genetic differences, the use of different mouse strains can also influence oocyte counts. Additional computational approaches have been developed for histomorphometric evaluation and include the automated detection of oocytes using the fractionator approach, automatic counting using computational algorithms, and 3D reconstruction of histological images to prevent multiple counts of the same oocyte[31–36]. Even with these improvements added to histomorphometric evaluation, the technique is relatively labor-intensive, particularly for large-scale and high-throughput studies. The data collected may not be reproducible and comparable between studies due to differences in counting schemes, computer algorithms, and software used.

Recently, accelerated by the development of new medium-resolution multiphoton and light sheet microscopy and optical tissue clearing methods, 3D modeling and analysis techniques for intact ovaries are becoming the method of choice to efficiently quantify oocyte numbers and study protein localization and dynamics[37,38]. These 3D methods are typically advantageous compared to histological methods as tissues and organs are better preserved and kept intact. Moreover, 3D analysis and modeling provide additional insights into function and interactions within and between cell niches or substructures within the organ that may be missed in 2D analysis.

3D analysis of whole organs requires optimization of fixation, immunostaining, and optical clearing protocols for individual organs, such as ovaries, without tissue distortion or damage. Additional optimization of sample mounting for imaging is required for high-resolution microscopy and may depend on the imaging platform available. Finally, imaging of the whole intact ovary generates a large amount of data for subsequent computational analyses. Therefore, there is a need to develop standardized 3D methods for counting oocytes for comparative studies and across developmental stages.

This protocol uses standard immunostaining and previously reported clearing protocols, focusing on a simple, user-friendly, and high-throughput approach[38–41]. The protocol is optimized to analyze large numbers of prenatal and postnatal ovaries up to postnatal day 28 (P28) and varying sizes of ovaries from different mouse genetic backgrounds. The immunostaining steps are similar for all stages; however, the clearing protocols differ for pubertal ovaries due to their larger size, ScaleS4(0) and CUBIC for small and large ovaries, respectively[40,41]. Further, whole-body perfusion is performed in P28 mice before fixation to prevent autofluorescence from blood cells. A multiphoton microscope was built on the Leica DIVE/4Tune platform as an alternative to light sheet microscopy to acquire images, and IMARIS 3D Visualization and Analysis software with

various analytical tools was chosen for this protocol. This protocol is simple to follow and less hands-on, hence time-saving. Moreover, oocyte quantification is relatively quick, depending on the size of the ovary and arrangement of oocytes.

PROTOCOL:

All mice used were of the genetic strain C57BL/6J (see the **Table of Materials**). This strain has been fully sequenced and is standard for many studies on ovarian structure and function. Mice were housed according to NIH guidelines, and procedures performed were approved by the Institutional Animal Care and Use Committee of The Jackson Laboratory. Reagents and compositions used in this protocol are listed in **Table of Materials** and **Table 1**, respectively.

1. **Preparation of reagents**

1.1. Fixative: Prepare 4% paraformaldehyde (PFA) in 1x PBS. For example, for 24 samples (0.5 mL/sample = 12 mL total volume), add 3 mL of 16% PFA electron microscopy-grade to 9 mL of 1x PBS.

1.2. Permeabilization buffer

1.2.1. Measure polyvinyl alcohol (PVA) into a 250 mL plastic beaker containing 1x PBS the day before the permeabilization buffer is needed. Stir the solution overnight to allow PVA to dissolve completely.

1.2.2. Add sodium borohydride to the dissolved PVA and allow the mixture to homogenize for approximately 3–5 min. Expect the solution to foam.

1.2.3. Add Triton X-100 to the solution and use the buffer once the Triton X-100 is dissolved.

NOTE: PVA takes a long time to dissolve (at least 3 h), and the penetration of the antibody depends on how well it dissolves. For larger ovaries, it is crucial to dissolve PVA completely.

1.3. Blocking buffer

1.3.1. Measure bovine serum albumin (BSA) into a beaker with 1x PBS. Stir the solution until the BSA is dissolved.

1.3.2. Add glycine, Triton X-100, Penicillin-streptomycin, and sodium azide. Stir until the solution homogenizes. Transfer the buffer into a bottle and store at 4 °C. Add normal goat serum before use.

1.4. Washing buffer: Measure PVA into a beaker containing 1x PBS. Stir the solution overnight to allow the PVA to dissolve. Add Triton X-100 and sodium azide. Once the buffer is mixed, store it at 4 °C.

1.5. ScaleS4(0) solution (pH 8.1): Dissolve D-sorbitol in PBS in a beaker with stirring at ≤100 °C. Add urea to the solution, and once the urea dissolves, turn off the heat and allow the solution to stir until completely dissolved. Add glycerol and dimethyl sulfoxide, and stir until the solution homogenizes. Store the solution at room temperature in the dark.

NOTE: ScaleS4(0) solution must be made fresh on the first day of clearing ovaries.

1.6. ScaleCUBIC-1 solution

1.6.1. Dissolve urea in a beaker containing PBS with stirring at temperature ≤100 °C. Measure *N,N,N',N'*-tetrakis(2-hydroxypropyl)ethylenediamine into a separate beaker, then add the dissolved urea, and stir at a temperature of ≤100 °C until the reagents completely dissolve. Once all the reagents are in solution, turn off the heat, and cool at room temperature. Store in the dark.

1.6.2. Degas the solution by transferring it into a filtering flask. Attach the flask to a vacuum with tubing, cover the flask, and turn on the vacuum until bubbles in the solution disappear. Use the solution after this degassing.

NOTE: The solution can be stored in the dark to use for up to a month.

1.7. Sucrose solution: Dissolve sucrose in 1x PBS; then degas the solution before use.

NOTE: Prepare the solution freshly before use.

1.8. ScaleCUBIC-2 solution

1.8.1. Dissolve sucrose in a beaker containing PBS with stirring at a temperature ≤100 °C. Add urea and stir at a temperature of ≤100 °C until the urea dissolves. Turn off the heat.

1.8.2. Add triethanolamine and Triton X-100. Stir until the solution homogenizes. Allow the solution to cool to room temperature and store in the dark. Degas the solution before using.

NOTE: The solution can be stored in the dark to use for up to a month.

2. Dissection and fixation of prenatal ovaries (**Figure 1A**)

2.1. Mate adult females (≥8 weeks) and males according to the approved institutional protocol. Check for vaginal plugs every morning.

NOTE: The morning of a vaginal plug is designated as 0.5 days post coitum (d.p.c) or E0.5.

2.2. On the day of dissection, prepare 4% paraformaldehyde (PFA) and aliquot ~0.5 mL into microcentrifuge tubes, placed on the bench side (~4 per pregnant female).

NOTE: PFA is a hazardous substance and must be handled under a chemical hood.

2.3. Prepare three 100 mm plates containing ~10 mL of 1x phosphate-buffered saline (PBS) for each pregnant female (for harvesting uterus, for dissecting mesonephros-ovary complex, and isolating ovaries).

2.4. Euthanize pregnant females that carry embryos of the preferred developmental stage and proceed to dissection. Euthanize no more than 1–2 females at a time. Use an approved protocol for the euthanasia of pregnant mice (e.g., CO_2 exposure followed by cervical dislocation).

2.5. Once a female is euthanized, spray the abdomen with 70% ethanol. Using forceps, lift the abdominal skin and use scissors to make a V-shape incision through the abdomen and body wall. Cut along the two sides of the incision and peel the skin back to expose the internal organs and fetuses in the uterus.

2.6. With forceps and scissors, cut and separate the uterus with the fetuses from the abdominal fat and ovarian arteries and veins. Remove the uterus and place it into a 100 mm plate containing 1x PBS. Release the fetuses into PBS by cutting the uterine wall and puncturing the yolk sac. Cut the umbilical cord.

NOTE: For fetuses younger than 15 days in gestation, euthanasia of the mother and removal from the uterus ensures rapid death of the fetus. Fetuses older than 15 days in gestation to birth must be euthanized by decapitation.

2.7. Transfer a fetus into a new plate with fresh 1x PBS. To decapitate an E15.5 fetus, delicately pin the two hindlimbs apart on the plate with forceps to immobilize the fetus. Using a second pair of forceps held in the dominant hand, hold the neck between the forceps prongs and squeeze to cut off the head of the fetus, or use scissors to cut the neck.

2.8. With the dominant hand forceps, cut below the forelimbs and gently pull the upper body away. Next, insert one endpoint of the dominant hand forceps into the peritoneal cavity vertically into the opening of the abdominal region while the other endpoint of the forceps remains outside. Close the forceps, pinch the body wall to cut it, and expose the internal organs.

2.9. With the same forceps, gently remove the organs, including the intestines and liver, until the kidney and the reproductive organs become visible. Determine the sex of the fetus: at E15.5, ovaries have an elongated sausage-like shape while the testes are oval.

NOTE: At earlier stages, genotyping may be needed to determine the sex.

2.10. Using one pair of forceps, hold the female fetus down and use the other forceps to grasp each mesonephros-ovary complex and gently separate it from the kidneys and the Müllerian ducts. Place the ovaries in a new plate with 1x PBS, leave the mesonephros attached, but remove the surrounding tissues to ensure that the ovaries are exposed. Place both ovaries into ~0.5 mL of 4% PFA in microcentrifuge tubes and fix at 4 °C overnight. The next day, replace PFA with 70% ethanol.

2.11. For the dissection and fixation of E18.5 ovaries, separate the fetuses from the uterus as described above and then follow the protocol for prepubertal pups described in section 3 (**Figure 1B**).

3. Dissection and fixation of prepubertal ovaries (**Figure 1B**)

3.1. Prepare 4% PFA and aliquot ~0.5 mL into 1.5 mL tubes and place them on the bench side (~one tube per pup). Prepare 35 mm plates with 1x PBS (~one per pup). Euthanize the pups using the approved institutional protocol.

NOTE: Decapitation is the preferred method of euthanasia for mice 8 days of age or younger. Neonatal mice can be decapitated using either 3–4" dissecting scissors or 5–7" Mayo scissors.

3.2. Determine the sex of pups by measuring the anogenital distance, which is greater in males than in females. Use sharp decapitation scissors to decapitate female pups. Place the body, open-cut side down, on a paper towel to drain the blood (~5–10 s).

3.3. Secure the pup on its back by placing a pin in the paw pad of each foot. Spray the abdomen with 70% ethanol. Use forceps to hold the pup's skin away from the body and use scissors to make a small V-shaped incision in the skin of the lower abdomen.

3.4. Insert the scissors into the incision under the skin and cut along both sides of the abdomen. Use the forceps to gently peel back the skin and reveal the lower abdomen. Gently move the intestine up and locate the uterine horns next to the bladder. Follow each uterine horn towards the kidney and locate the ovary with surrounding adipose tissue below each kidney.

3.5. To dissect the ovaries, hold the uterine horn below the ovary and oviduct with one pair of forceps (forceps A, **Figure 1B**) and gently lift it away from the body. Using another pair of forceps (forceps B), gently grab underneath the first pair of forceps so that the ovary and oviduct in the adipose pad are visible above the second pair of forceps. Then, cut below the second pair of forceps with scissors or carefully pull to detach the ovaries and attached tissues.

3.6. Place the isolated organs in a plate with 1x PBS. Trim away the extra adipose tissue, oviduct, and uterine horn to clean and isolate the ovary. Delicately open the bursa surrounding the ovary and expose the whole ovary.

3.7. Trim the bursa membrane without damaging the ovary and leave tissue around the hilum (ligament-like structure between the ovary and the reproductive tract) to handle the ovary, as shown in **Figure 1B**, P5. Once the ovaries are trimmed, place them in 4% PFA and fix the ovaries at 4 °C overnight. The next day, replace 4% PFA with 70% ethanol and store the ovaries at 4 °C until the immunostaining protocol step.

4. Perfusion, dissection, and fixation of pubertal ovaries (**Figure 1C**)

4.1. Perfuse mice according to institutionally approved protocols with the mouse under deep anesthesia in a chemical fume hood. Prepare the perfusion equipment and reagents. See the detailed protocol at [42].

NOTE: Perfusion is a terminal euthanasia procedure that replaces the blood throughout the vascular system with a tissue fixative.

4.2. Weigh a pubertal female mouse (P28) and record the mouse's weight (typically between 13 g to 15 g). Calculate the amount of the approved anesthesia agent to be used.

NOTE: Here, 0.35 mL of tribromoethanol per 10 g of body weight was used in this protocol.

4.3. Use a 10 mL disposable syringe with a 20 G needle to fill the syringe with the approved anesthetic agent. Replace the 20 G needle with a 26 G x 3/8 needle.

4.4. Carefully restrain the mouse by scruffing the dorsal neck skin with one hand. Turn the mouse over to expose the abdomen. Inject the previously calculated amount of anesthetic into the peritoneal cavity. Place the mouse in a container with a cover until the anesthesia takes effect (i.e., the mouse no longer moves).

4.5. Once the mouse stops moving, gently pinch its feet to check that there is no response and ensure that the mouse is fully anesthetized before initiating the perfusion. Place and secure the mouse on its back by gently pinning all four legs through the paw pads onto a board. Ensure that the legs are pinned in a relaxed position, not overstretched.

4.6. Spray the mouse with 70% ethanol from the abdomen to the chest region. Use forceps to gently pinch and lift the abdominal skin and then use scissors to make a small V-shaped cut through the skin and body wall.

4.7. Lift away the skin flap from the body cavity and insert the scissors below the skin and body wall. Cut the skin and body wall straight up toward the head to the edge of the thoracic cavity at the sternum.

4.8. Open the thoracic cavity by carefully cutting the ribs on both sides of the sternum to just below the scapula. Take care not to puncture the lungs below the rib cage. Grab the skin/rib flaps with forceps and pin them to expose the internal organs.

4.9. Gently trim any tissue, such as the thymus, that may obstruct clear access to the heart. Expose all organs, including the gastrointestinal tract, to allow visual confirmation that the whole body is perfused, including the lower abdomen.

4.10. Use dissection scissors to snip the right atrium of the heart and release blood from the system. Gently hold the heart with forceps and insert a perfusion needle (connected to a peristaltic pump controller) into the left ventricle.

4.11. Pump ~10 mL of PBS, with gentle but constant pressure, until tissues such as the liver, kidneys, and reproductive tract (**Figure 1E,F**) turn from pink to white. Next, replace the PBS with freshly made 1% PFA and continue perfusion with approximately 10 mL of PFA or until twitching occurs in the lower body of the mouse (e.g., tail).

NOTE: These fixation tremors indicate successful perfusion.

4.12. Once perfusion is completed, locate the fat pad with the ovaries below the kidney and gently dissect the entire reproductive tract, including the fat pad, ovaries, and uterine horns, and place the tract in a vial with 4% PFA. Fix the ovaries at room temperature overnight (~16–24 h). Then, replace the 4% PFA with 70% ethanol for at least one day and trim the ovaries (**Figure 1E,F**), as described above, before starting the immunostaining protocol.

5. Whole-mount ovary immunostaining (**Figure 2A**)

NOTE: Practice sterile techniques during the immunostaining protocol, especially when changing buffers, to prevent contamination during extended incubation periods.

5.1. Perform all immunostaining steps in a 24-well plate, as shown in **Figure 2A**. Adjust reagent volumes for other formats. Change buffers carefully to avoid losing small prenatal and prepubertal ovaries.

NOTE: Other formats, such as 48- and 96-well plates, can be used, but the deeper wells and narrower openings make it difficult to aspirate buffers without losing or damaging ovaries.

5.2. Day 1

5.2.1. Pipette 1 mL of PBS/well into the number of wells needed in a clean 24-well plate. Cut off the tip of a 200 µL pipette tip to make a wide opening and use it to gently transfer prepubertal ovaries from 1.5 mL tubes with 70% ethanol into the wells. For pubertal ovaries, use a 1000 µL pipette tip with the tip cut off for the transfer.

NOTE: The wider opening of the tip prevents tissue damage during transfer.

5.2.2. Once all the samples are transferred into the wells, use a new tip to aspirate the PBS and replace it with fresh 0.8 mL of PBS/well. Incubate the samples at room temperature on a shaker at ~100–150 rpm overnight. Start preparation of the permeabilization buffer (see **Table 1** and section 1).

NOTE: The new tip prevents ovaries from sticking to the tip, and the PBS incubation step allows the ovaries to equilibrate in PBS and rehydrate before staining.

5.3. Day 2

5.3.1. Finish preparation of the permeabilization buffer. Aspirate PBS from the wells and replace it with 0.8 mL of the permeabilization buffer per well. Place the plates back on the shaker and incubate the samples at room temperature for 4 h.

5.3.2. After 4 h of incubation, completely aspirate the permeabilization buffer and replace it with 0.5 mL of blocking buffer (see **Table 1** and section 1). Seal the plate with parafilm to prevent evaporation, place in a securely covered container on a shaker, and incubate the samples with gentle agitation in blocking buffer overnight (16–24 h) at room temperature.

5.4. Day 3

5.4.1. Prepare the primary antibodies by dilution in blocking buffer. For visualizing oocytes, use oocyte markers, e.g., rat anti-germ cell nuclear acidic peptidase (GCNA)/TRA98 for both prenatal and prepubertal ovaries and rabbit anti-DEAD-box helicase 4 (DDX4)/mouse vasa homologue (MVH) for both prepubertal and pubertal ovaries. For quantifying LINE-1 ORF1p expression in prenatal ovaries, use rabbit anti-LINE-1 ORF1p or another available antibody.

NOTE: GCNA/TRA98 signal is not detectable in the pubertal ovaries.

5.4.2. Aspirate the blocking buffer from the samples and replace it with 0.5 mL of diluted primary antibodies. Seal the plate with parafilm to prevent evaporation. Place the plates in a container with a cover to prevent the drying up of samples during incubation. Place the container on the shaker and incubate the samples for 3–4 days at room temperature.

5.5. Day 7

5.5.1. Gently remove the parafilm from the plates and aspirate the primary antibody mixture from the samples. Store the primary antibody mixtures at 4 °C (for up to a month or three uses) and reuse them later by supplementing with fresh antibodies (e.g., 2 µL of fresh antibody aliquot per 5 mL of the previously used mixture).

5.5.2. Add 1 mL of washing buffer (see **Table 1** and section 1) per well to the samples and gently rock the plates for a few seconds to rinse away the residual antibodies. Carefully aspirate and

replace the washing buffer with 0.8 mL of fresh washing buffer and shake the plates at room temperature overnight.

5.6. Day 8

5.6.1. Aspirate the overnight washing buffer, replace it with 0.8 mL of fresh washing buffer, and shake at room temperature for 2 h. Repeat the washing step with fresh washing buffer for another 2 h.

5.6.2. After the last wash, replace the washing buffer with 0.5 mL of secondary antibody mixes diluted in a blocking buffer, e.g., goat anti-rat Alexa Fluor 555 and goat anti-rabbit Alexa Fluor 647 at 1:1,000 dilution. Prepare the secondary antibody mixture fresh for each immunostaining experiment.

5.6.3. Seal the plate with parafilm to prevent evaporation during incubation. Incubate the samples at room temperature in the dark or in plates covered with aluminum foil with gentle agitation for 3 days.

NOTE: This step and all subsequent steps take place in the dark or with aluminum foil wrap.

5.7. Day 11

5.7.1. Aspirate the secondary antibody mixture and perform an initial wash with 1 mL of washing buffer. Gently rock the plates for a few seconds to rinse away the residual secondary antibodies.

5.7.2. Aspirate the washing buffer, replace it with 0.8 mL of fresh washing buffer, and incubate the samples at room temperature for 2 h with shaking, protected from light. Repeat the washing step 2 times for a total of 3 washes. After the third wash, proceed to the clearing step (section 6).

6. Clearing of immunostained whole-mount ovaries (**Figure 2A**).

NOTE: Perform all clearing steps in the dark by wrapping the plates in aluminum foil or placement in opaque containers. The clearing steps differ for prepubertal and pubertal ovaries.

6.1. Day 11 [Prenatal and prepubertal ovaries are cleared in a one-step protocol]

6.1.1. After the last wash, aspirate the washing buffer and replace it with 0.8 mL of freshly made ScaleS4(0) solution (see **Table 1** and section 1). Seal the plate with parafilm and incubate the samples in the dark with shaking at room temperature for three to four days before imaging.

6.1.2. Replace the ScaleS4(0) solution with a fresh solution daily if needed; Take care while replacing the solutions, as cleared ovaries become transparent and are difficult to see. After clearing, proceed to sample set up and imaging (section 7).

NOTE: Changing solutions did not significantly improve image quality. Daily changes increase the likelihood of losing small and mostly transparent samples.

6.2. Days 11–15 [Pubertal ovaries are cleared in a two-step protocol]

6.2.1. After the last immunostaining wash, aspirate the washing buffer and replace it with 0.8 mL of ScaleCUBIC-1 (see **Table 1** and section 1). Seal the plate with parafilm and gently shake samples at 37 °C for 3 days in the dark. Replace the ScaleCUBIC-1 solution with the fresh solution daily.

6.2.2. On day 15, wash the samples 3 times for 10 min each time in 0.8 mL of PBS at room temperature with gentle shaking. Replace the PBS with 0.8 mL of degassed 20% sucrose prepared freshly with PBS. Shake gently at room temperature for 1 h.

6.2.3. Replace the 20% sucrose solution with 0.8 mL of ScaleCUBIC-2 Solution (see **Table 1** and section 1), seal the plate with parafilm, and shake gently at room temperature with daily changes of the ScaleCUBIC-2 Solution. Clear for 4–5 days and proceed to image. Take care when exchanging solutions to avoid sample loss as cleared ovaries are transparent and difficult to see. Proceed to sample set up and imaging (section 7).

7. Sample setup and imaging with a multiphoton microscope

NOTE: All steps described below were performed with a Leica DIVE/4TUNE/FALCON with two tunable mode-locked Ti:Sapphire multiphoton lasers with a pulse duration of 120 fs with a multi-immersion 16x/NA0.6 objective (immersion liquid = glycerol) with a maximal working distance of 2.2 mm. See the **Table of Materials** for details about the image acquisition software. **Supplemental Table S1** and **Supplemental Figure S1** show the settings used for this protocol. For other imaging platforms, consult with the microscopy core or follow the manufacturers' specifications/recommendations.

7.1. Sample setup

7.1.1. Prepare the setup for mounting the samples. For example, use a sticky and flexible silicone gasket to create an adhesive well. Place the adhesive well on one 25 mm x 25mm No. 1.5 micro coverslip to create a well in which the ovaries will be placed (**Figure 2B**).

NOTE: A gasket of 1 mm thickness accommodates all sizes of ovaries. This setup is recommended as it eliminates ovary movement during imaging, which can occur when ovaries are placed in mountant in a glass-bottom dish.

7.1.2. Using a pipette tip with the tip cut off (20 µL for prenatal and prepubertal), transfer the ovaries with ~5–10 µL of ScaleS4(0) solution into the middle of the adhesive well as shown in **Figure 2B**. For pubertal ovaries, use a 200 µL pipette tip with the tip cut off far enough to transfer the ovaries. Add ~15–20 µL of the ScaleCUBIC-2 Solution into the middle of the adhesive well.

NOTE: Too much solution may cause leaking onto the microscope stage, and too little solution will result in poor image quality.

7.1.3. Once the ovaries are transferred into individual wells with a drop of clearing solution, gently place another cover glass on the adhesive well, press to create a seal, and keep the samples in place in a small pool of clearing solution sandwiched between the two coverslips (**Figure 2B**). For imaging, place the coverslip "sandwich" in a 3D printed microscope adapter slide (e.g.,[43]).

NOTE: Adhesive wells are reusable after deconstructing the "sandwich" and washing with water.

7.2. Imaging (**Supplemental Table S1** and **Supplemental Figure S1**)

7.2.1. Turn on the microscope and software according to the guidelines of the microscopy core or the manufacturer. Place the mounted samples onto the microscope stage and look through the eyepiece to locate the sample lit with a low-power LED fluorescence lamp.

7.2.2. Once the samples are located, turn on the laser(s) and assign each detector to a specific Alexa Fluor dye/marker. For multiple lasers, allow for sequential image acquisition. Acquire the whole stack prior to switching lasers.

NOTE: For this protocol, one laser was used for the image acquisition of both 555 nm and 647 nm fluorophores.

7.2.3. Set up the parameters for image acquisition according to the microscopy core's or the manufacturer's specifications. Use bidirectional image acquisition, if available, to reduce the scanning time and improve efficiency. Adjust other settings, including the **line average** (1), **frame average** (1), and **frame accumulation** (1).

NOTE: Bidirectional image acquisition allows lasers to scan in both directions as they move on the X-axis.

7.2.4. Set up the Z-Stack by identifying the beginning (bottom of the sample/bottom glass cover) and the end position (top of the sample/top glass cover). Select a **Z-step size** of 2 µm for prepubertal ovaries and 5 µm for pubertal ovaries.

7.2.5. Activate the Z-compensation feature, and within this feature, activate the **excitation gain**. Set the Z-compensation for the bottom and top of the sample by selecting a **laser intensity** for both the bottom (low intensity) and top stack (high intensity). See **Supplemental Figure S1**, Linear

Z-compensation, where excitation gain box is selected, and laser intensity for the bottom (0) and top (347.75) is set as 10 and 12, respectively.

7.2.6. Use the **tiling mode** for larger samples that cannot be captured in a single field of view. Activate the **image navigator** and indicate the **number of tiles** needed to capture the entire sample using the **rectangular marking tool**.

7.2.7. Start the image acquisition. For images with multiple tiles, start image acquisition with the **navigator** to capture all tiles. Once the image acquisition is completed, first **save** all images, and if multiple tiles were acquired, then run the **mosaic-merge tool** to merge the tiles into a single image.

7.2.8. Save the merged files into a separate project folder to make it easier to work with the Gigabyte-sized images. Transfer the files for image processing with 3D image visualization and analysis software. **Figure 3** shows representative images taken at different stages with two markers (GCNA and DDX4).

8. Image processing

NOTE: All steps described below were developed and performed using IMARIS 3D image visualization and analysis software.

8.1. Import the image(s) into the 3D image visualization and analysis software and, if needed, convert the files from the original format (e.g., .lif, .czi, .lsm, .lei, .oib, .oif, .nd2) to the .ims format.

8.2. If needed, process the images with the gaussian filter to reduce pixelation (**Figure 4A**). Using the **3D view** feature, position the image and deselect the **frame option** (to remove the frame).

NOTE: There are other optional filters, that can also be used to decrease pixelation and reduce background intensity.

8.3. Enlarge the image to a specific scale and use the **Snapshot feature**. Set the preferences as follows: select **300 DPI**, **save as TIFF Image**, and **Transparent Background**. Take a snapshot of the image and save it. **Figure 3** shows complete assembled images.

9. Oocyte Quantification

NOTE: Whole ovary immunofluorescence and 3D image visualization and analysis can be used for the estimation of oocyte numbers in whole ovaries (**Figure 3** and **Figure 4**) using the **Spot feature.** The GCNA signal can be used to quantify oocytes in prenatal and prepubertal ovaries, as shown in **Figure 4** (P5). In pubertal ovaries, use the DDX4 signal to quantify two oocyte populations in non-growing follicles ("ring-like" structure, closed arrow) and growing follicles (large structures, open arrow, **Figure 4**, P28).

9.1. Determine the size of oocytes that will be used as a parameter to quantify oocytes with the **Spots** feature in step 9.2.

9.1.1. Open the image and select the **Slice** option to open the Z-stack image.

9.1.2. Select the **Line** option in the **Measure** panel and measure the distance by drawing a line from one edge of an oocyte/marker to the other edge at the widest point to determine the XY diameter of the oocyte type/size to be counted. Move through the stack and obtain the range of diameters for multiple oocytes of the same type. Use the shortest length as the size selection criterion for oocyte counts.

9.2. **Spots** feature: Select the **3D View** option and activate the **Add new Spots** function in the **Scene** panel to open the **Algorithm** panel. Deselect all the algorithm settings as the size selection filter with the oocyte size obtained in step 9.1 will be used.

9.2.1. Click on the **single forward arrow** to move to the **Source Channel**. Select the **Channel** with the preferred marker and type in the **Estimated XY Diameter** obtained in step 9.1. For example, use an estimated XY diameter of 7 µm for prenatal oocytes and 11 µm for P5 oocytes (GCNA = green signal; **Figure 3** and **Figure 4A**).

9.2.2. Use 30 µm for the DDX4 signal to estimate the number of oocytes in growing follicles in P5 ovaries (DDX4 = magenta signal; **Figure 3** and Figure **4A**). For pubertal ovaries, use the DDX4 signal for oocyte quantifications. For example, use XY diameters of 15 µm and 80 µm to identify oocytes within non-growing follicles and growing follicles, respectively, as shown in **Figure 4A**.

NOTE: The size selected may vary due to image acquisition criteria and the type of microscope used. The selection may also vary among genetic strains as ovaries with more oocytes will require smaller size selections for better automated oocyte detection.

9.2.3 After size selection, activate the **Model PSF-elongation** and **Background subtraction**, which are automatically determined. Select the **single forward arrow** to move to the **Filter Spots** panel. Add the **Quality** filter and determine a threshold. To ensure the accurate estimation of oocyte numbers, enlarge the image as the threshold is adjusted to choose a threshold value that selects most of the oocytes. Click on the **double arrow** to finish automated counts.

9.2.4. Manually check the selected oocytes using the **Edit** tab to select missed oocytes or deselect non-oocyte particles selected by the automatic threshold. Record the data in the **Statistics** tab under the **Overall** tab for further analysis.

NOTE: The parameters used for counting the spots can be saved and used for another sample set but it is recommended to do a manual check before running batch analysis.

9.2.5. To store the parameters, click on the **Creation** tab and click on **Store Parameters for Batch**.

NOTE: Nuclear markers (GCNA+ oocytes, **Figure 4A**) are easily identified by the spot feature and may not require much manual adjustment. However, the cytoplasmic marker (DDX4+ oocyte, **Figure 3 (**P28, closed arrow) and **Figure 4A**) will require more manual adjustment to ensure the identification of the correct size/type of oocytes.

10. Quantifying protein expression in ovaries

NOTE: There are several ways to quantify oocyte expression of specific markers using both the **Spots** feature (section 9 and step 10.1) and **Surfaces** feature (step 10.2). The **Spots** feature can be used for proteins with distinct localization patterns such as nuclear markers (GCNA), and the **Surfaces** feature can be used for proteins with non-uniform localization patterns as shown in **Figure 5A** where LINE-1 ORF1p intensities in E15.5 and E18.5 ovaries were measured. To calculate and compare the intensity of the protein of interest between two samples (e.g., timepoints, treatments, or genotypes), collect images with the same properties. Use samples with a more intense signal to determine the parameters that can be stored and used for the other samples.

10.1. To obtain the protein expression with the **Spots** feature, first identify oocytes as highlighted (section 9).

10.1.1. Then under the **Spots** feature, select the **Statistics** tab, followed by the **Detailed** tab. Click on the **down arrow** and select **Specific Values**, which will open another tab beneath it containing different measurements. Select the **Intensity Mean** of the channel used for the surface generation (or select other intensity measurements such as the **Intensity Median**).

10.1.2. To obtain the combined/average statistical information, select the **Average Values** criterion. Once done, export and save data for further analysis.

10.2. To obtain the protein expression with the **Surfaces** feature, open the image, select the **3D View** option and activate the **Add new Surfaces** function in the **Scene** panel to open the **Algorithm** panel. Deselect all the algorithm settings if not needed and click on the **single forward arrow** to move to the **Source Channel**.

10.2.1. Select the **Channel** with the antibody signal to measure. Other properties to select are user-specific options. Here, the LINE-1 signal was used as a marker. The **Surfaces Detail** and **Background Subtraction (Local Contrast)** values were kept at default values of 1.42 and 5.33, respectively.

10.2.2. Click on the **forward arrow** to move to the **Threshold** panel. Choose a threshold value that is comparable in both samples (e.g., here, LINE-1 expression in E18.5 was used to choose a threshold). Select **Enable** with a default **Seed Points Diameter** of 7.10 (this value was found optimal for the images but may depend on the expected pixel-size of features).

10.2.3. Click on the **forward arrow** to move to the **Filter Surfaces** panel. Use a **Quality** filter was used, and base the value, as with the **Threshold** value, on the expression of the proteins in both ovary samples. Once the filter property is selected, click on the **double forward arrow** to complete the generation of the surface.

10.2.4. To obtain the intensity values, select the **Statistics** tab, followed by the **Detailed** tab. Click on the **down arrow** and select **Specific Values**, which will open another tab beneath it containing different measurements.

10.2.5. Select the **Intensity Mean** of the channel used for the surface generation (or select other intensity measurements such as the **Intensity median**).

10.2.6. To obtain the combined/average statistical information, select the **Average Values** criterion. Once done, export and save the data for further analysis (**Figure 5C**).

11. Estimation of total oocyte numbers in damaged ovary with computational correction

NOTE: If a minor ovary damage occurs during dissection, it may be possible to computationally estimate total oocyte count. It is recommended to use intact ovaries from the same strain and developmental stage for oocyte number estimation as shown in **Figure 6**. Simulations performed with ovaries at E15.5 indicate that correcting for a ≥30% loss results in a significant deviation from actual numbers (**Figure 6C**).

11.1. Open images of intact ovaries with IMARIS and select the **Frame** feature. Under the **Frame Settings**, select the **Box**, **Grid**, **Tickmarks**, and **Axis** labels. Under the **Position X/Y/Z** tab, select **200 µm** to generate tickmarks with 200 µm spaces in all X/Y/Z positions.

NOTE: The tickmarks create a grid/ruler in X, Y and Z planes to identify oocytes within a specific region.

11.2. Activate the **Spots** feature to identify the oocytes as highlighted in section 9 (**Figure 4**). Create a 3D model using the oocytes identified in all intact ovaries being used for the simulation by selecting **Sphere** under the **Points Style/Quality** tab in the **Spots** feature.

NOTE: The **Pixel Width** can also be changed under the **Points Style/Quality** tab.

11.3. With the box generated in step 11.1, align the 3D models of the intact ovaries in the same orientation as shown in **Figure 6A**.

11.4. Using the 200 µm tickmarks (step 11.1), select oocytes that fall within 50% of the volume of each ovary. Click on the **Spots** feature and select **Edit Labels** to classify the oocytes that fall within the 50% region by color, as shown in **Figure 6A**.

NOTE: Once oocytes are classified in a region, the number of oocytes that fall within each class will be provided.

11.5. Zoom into the 50% region and change the **tickmarks** from **200 µm** to **50 µm** to make a smaller ruler for oocyte identification. Maintain the zoom % in all images. With the 50 µm tickmarks as a guide, divide the 50% region into five equal parts.

NOTE: Oocytes within each part will represent 10% of the volume as highlighted in **Figure 6A**, where an intact ovary shows oocytes in the top half of the ovary classified by five different colors with each color representing oocytes within a 10% volumetric region.

11.6. Record the oocyte numbers in each 10% region as shown in **Figure 6A,B**. Calculate the average number of oocytes for 10, 20, 30, 40, and 50% increments.

11.7. Use the highlighted in steps 11.1 to 11.6 to obtain oocyte numbers in the damaged partial ovary. Position the damaged ovary in the same orientation as the intact ovaries and estimate missing volume/percentage as described above.

11.8. To estimate the total oocyte number in the **whole** ovary, add the average number of oocytes calculated for a similar volume to the number obtained from the partial ovary (**Figure 6B**).

REPRESENTATIVE RESULTS

Immunostaining and imaging of the whole ovary enables the visualization and quantification of oocytes or protein expression in ovaries at different developmental stages using the same technique and markers (**Figure 3**). This protocol was developed for a large-scale project in which analysis of ovaries at multiple stages and from multiple mouse strains was required. Here, we present data gathered for the C57BL6/J strain, a standard strain for genetic analysis. The technique presented here is straightforward, results can be obtained within 14–19 days (**Figure 2D**) and can be used for ovaries from prenatal, prepubertal, and pubertal females (**Figure 1** and **Figure 2A,B**).

This approach was used to study the dynamics of the oocyte loss that occurs naturally during the formation of the ovarian oocyte reserve. In many organisms including the mouse, oocyte numbers are thought to peak during fetal life around the time that oocytes enter meiosis ~E13.5. Oocyte numbers decrease due to the still-not-fully-understood process of fetal oocyte attrition (FOA) (from ~E15.5 to E18.5), which has been mechanistically linked to the expression of the retrotransposon LINE-1[20,21]. More oocytes are eliminated after E18.5 to P0 due to the elimination of abnormal oocytes by a meiotic quality checkpoint[22,23]. To investigate these processes using this protocol, we immunostained and imaged ovaries at different developmental stages using DDX4 and GCNA as oocyte markers as shown in **Figure 3**.

Small oocytes expressing GCNA and DDX4 are seen from E15.5 onwards and they represent oocytes during MPI or arrested at dictyate within primordial follicles. Larger growing oocytes with strong DDX4 expression are detected already in P2 ovaries where they most likely represent the first wave of follicles[44]. Increasing numbers of larger oocytes are seen in P5 and P28 ovaries. Images obtained by multiphoton microscopy (**Figure 4A**) were processed using IMARIS software and 3D rendering was performed to identify small and larger growing oocytes based on the nuclear GCNA signal and the size delineated by the DDX4 signal (**Figure 4A** and **Video 1**). Oocytes were counted as described in the protocol and results are summarized in **Figure 4B.** In agreement with previous studies, we observed a significant oocyte loss from E15.5 to E18.5 (~32%) and E18.5 to P2 (~24%). By the time females reach puberty (P28), only ~30% of oocytes present at E15.5 have survived.

This method can be also used to observe the consequences of genotoxic treatments such as irradiation, which has been shown to completely eliminate the primordial follicle reserve within one week[23,38,45]. A significant visual difference is evident between the whole ovary treated with radiation and the untreated control in **Figure 3** (comparing P28 ovaries from treated and untreated females). In the P28 ovary without radiation exposure, we observed two oocyte populations labeled with DDX4; abundant small oocytes in primordial follicles (closed arrow); and larger oocytes of various sizes typically found in growing follicles (e.g., primary, secondary, and preantral) (**Figure 3**). In contrast, the ovary from a female exposed to 0.5Gy of γ-radiation at P7 is completely devoid of small oocytes in primordial follicles as previously observed in 2D sections. Interestingly, only larger oocytes of similar size survived radiation; these may be the first wave follicles already growing in the P7 ovary, as they are known to be resistant to radiation[46] (**Figure 3, P28**).

In addition to the quantification of oocyte numbers, this protocol can be used for immunostaining and quantitative analyses of other proteins involved in oocyte development. For example, we used antibodies against LINE-1ORF1p protein, an RNA-binding chaperone protein, produced by LINE-1 retrotransposons (**Figure 5**). Increase in the abundance of LINE-1 elements from E15.5 to E18.5 has been proposed to cause oocyte elimination[20,21]. Indeed, using multiphoton-captured images and signal intensity analysis in IMARIS, LINE-1 ORF1p levels were observed to increase significantly in oocytes during this time, which correlates with a significant drop in oocyte numbers as shown in **Figure 4B.**

In circumstances where a part of an ovary is damaged or lost, ovaries from the same strain and developmental stage can be used to computationally estimate the number of oocytes within the missing region as shown in **Figure 6**. Data from E15.5 ovaries were used for simulations to test the accuracy of computational corrections. Oocytes in ovaries with up to 30% tissue damage can be computationally estimated to have ≤10% deviation compared to oocytes in an intact ovary, suggesting that 3D ovary staining and modeling can be effectively used to salvage data from precious tissues. Simulations performed with ovaries at E15.5 indicate that correcting for a ≥30% loss results in a significant deviation from actual numbers (**Figure 6C**).

FIGURE AND TABLE LEGENDS:

Figure 1: Ovary dissection and perfusion from females from prenatal and postnatal stages. (**A–C**) Ovary dissection from different stages requires different techniques, which are depicted schematically to complement the descriptions in the video. (**D**) Ovaries at postnatal day 5 (P5) are much smaller than at P28, which necessitates a different clearing protocol as described in the protocol. (**E,F**) Proper perfusion of the ovaries is important to eliminate background staining from red blood cells. Non-perfused reproductive tracts and ovaries have pink hue while perfused organs will turn white. Abbreviation: RI = non-perfused reproductive tracts.

Figure 2: Immunostaining, clearing, and imaging of whole mouse ovaries. (**A**) Flow chart depicts shared and specific steps for immunostaining and clearing protocol for prenatal/prepubertal and pubertal ovaries. (**B**) Cleared ovaries are mounted in a drop of clearing solution in the middle of an adhesive well sandwiched between two cover slips. For imaging, the mounted samples are placed in a 3D printed adaptor slide. (**C**) Greyscale multiphoton images of non-perfused vs. perfused ovaries, immunostained with the oocyte marker DDX4, showing improved image quality and lower nonspecific staining after perfusion. The closed arrow indicates an oocyte with a thin layer of cytoplasmic DDX4 staining typical for primordial follicles, and the open arrows show larger oocytes within growing follicles. Asterisk indicates autofluorescence from blood vessels. (**D**) 3D renders from confocal vs. multiphoton images of P5 ovaries, immunostained with oocyte markers GCNA (green) and DDX4 (magenta), showing a significant spherical aberration from confocal microscopy and virtually none from multiphoton. Scale bars = 100 µm (**C, D**) and 50 µm (insets in **D**). Abbreviations: GCNA = germ cell nuclear acidic peptidase; DDX4 = DEAD-box helicase 4.

Figure 3: Representative 3D-rendered images of ovaries of different developmental stages. 3D renderings from multiphoton images of whole mount ovaries immunostained with GCNA (green) and LINE-1 ORF1p (blue) or DDX4 (magenta), in prenatal and postnatal ovaries, respectively. Individual channels are presented in grayscale to show nuclear and cytoplasmic signals. The white boxes outline regions magnified in the left bottom insets. Two different ovaries are shown for P28. The ovary from the control non-irradiated female (top) contains a large population of small oocytes in primordial follicles (see inset). In contrast, the ovary from the female irradiated at P7 with 0.5 Gy of γ-radiation (IR) is completely devoid of small oocytes in primordial follicles (see inset). The closed arrow indicates an oocyte with a thin layer of cytoplasmic DDX4 staining typical for primordial follicles, and open arrows show larger oocytes within growing follicles. Scale bars = 100 µm; 30 µm for P28 insets; 10 µm for all other insets. Insets contain magnified views of 3D-rendered images generated in IMARIS and may differ slightly from low-magnification images due to perspective. Abbreviations: Non-IR = control non-irradiated; IR = irradiated at P7 with 0.5 Gy of γ-radiation; GCNA = germ cell nuclear acidic peptidase; DDX4 = DEAD-box helicase 4; LINE-1 = long interspersed nuclear element-1.

Figure 4: Image processing, 3D display of oocytes, and quantification results. (**A**) 3D renders from multiphoton images (left) were processed in IMARIS using Gaussian filter (middle) and oocytes of small and large sizes were identified using the spot feature (right). P5 and P28 ovaries shown as example. Scale bars = 100 µm (P5); 10 µm (P5 insets); 300 µm (P28); 50 µm (P28 insets). (**B**) Small oocytes positive for GCNA were quantified in ovaries from different stages using spot

features (top). To illustrate decreasing numbers of oocytes during development, the average % of oocytes were calculated at each stage as compared to the average number present in the earliest stage counted at E15.5 (bottom). Note the large drop in oocyte numbers from E15.5 to E18.5. Data are presented as means ± SD. Statistical analyses were performed using GraphPad Prism software and analyzed by one-way ANOVA, and the significance was determined by Bonferroni's *post hoc* multiple comparison test. * $P \leq 0.05$; **** $P \leq 0.0001$; ns >0.05. Abbreviation: GCNA = germ cell nuclear acidic peptidase; ns = not significant.

Figure 5: Detection and quantification of the LINE-1 ORF1p expression in fetal oocytes. (**A**) 3D renderings from multiphoton images show LINE-1 ORF1p (blue) expression in E15.5 and E18.5 fetal oocytes (marked by green GCNA). (**B**) 3D surfaces generated in IMARIS using top row images in panel **A**. (**C**) LINE-1 ORF1p intensity analysis shows higher expression of LINE-1 ORF1p per oocyte at E18.5 than E15.5. Scale bars = 100 µm; 10 µm (panel **A** insets); 30 µm (panel **B** insets). Data are presented as means ± SD. Statistical analyses were performed using GraphPad Prism software and analyzed by Student's *t*-test, and the significance was determined by Mann-Whitney *U* test. $P \leq 0.0001$; ns >0.05. Abbreviations: GCNA = germ cell nuclear acidic peptidase; LINE-1 = long interspersed nuclear element-1.

Figure 6: Method for estimating total oocyte numbers in damaged ovarian samples with computational correction. (**A**) Model of GCNA-positive (green) E15.5 oocytes with five 10% regions highlighted in red, blue, gray, magenta, and brown in an intact ovary. Each succeeding image, after the intact ovary, represents a simulated ovary with 10% incremental regions missing up to 50%. (**B**) Schematic of computational method to estimate oocyte number in damaged sample. (**C**) Total oocyte numbers in simulated ovaries were compared to numbers in the original intact ovaries (considered 100%) and the difference is presented as % deviation. Simulation from six individual ovaries with 10–50% volume missing. Scale bars = 80 µm. Abbreviation: GCNA = germ cell nuclear acidic peptidase.

Video 1: **3D rendering and 3D modeling of oocytes in P5 ovaries.**

Table 1: Solutions and buffers.

Supplemental Figure S1: Image acquisition preferences.

Supplemental Table S1: Image acquisition settings.

DISCUSSION

This article presents a detailed 3D immunostaining and imaging protocol for prenatal and postnatal ovaries for high-throughput and comparative studies for germ cell quantification and protein localization. We developed this protocol to analyze oocyte numbers in ovaries (N=6–12) at six developmental time points in 10–16 different strains, where 2–4 24-well plates are typically processed at one time. This method can be adapted for other organs or cellular markers. For example, this protocol can be used to label and visualize somatic cells, such as granulosa cells in

the ovary, using appropriate antibodies, thus facilitating studies of somatic-germ cell interactions or development of other ovarian cell types.

One limitation of this protocol and antibody combination is the definitive identification of different follicular stages. DNA stains used in immunofluorescence and 2D imaging to identify follicular stages by layers of granulosa cell nuclei are insufficient for 3D approaches. The 4',6-diamidino-2-Phenylindole (DAPI) or Hoechst are rarely used for whole-organ staining due to limited light penetration and decaying signal in the middle of large tissue. Propidium iodide (PI) is a small molecule able to penetrate deep into the tissue but is difficult to capture on the multiphoton imaging system due to spectral overlap. Better resolution of follicular stages can be achieved by additional markers specific to granulosa cells such anti-Mullerian hormone (AMH) or FOXL2[47,48]. However, although these markers are helpful in differentiating larger growing follicles, they will not distinguish primordial from primary follicles. Until specific markers for these early stages become available, oocyte markers such as DDX4 or GCNA offer the best indicator of follicle development. Further, this protocol works for prenatal male gonads but has not yet been tested in the postnatal testis where its size may be the limiting factor. Critical issues are listed below for better visualization and quantification of germ cells in ovaries of varying sizes and the techniques and steps taken to ensure good quality immunostaining for downstream analysis are highlighted.

The first critical step is to prevent damage to the ovaries before and after fixation. Damaged ovaries may lack parts of the organ structure, affecting the oocyte numbers and skewing the experimental results. To prevent damage, extra somatic tissue is left attached to the larger ovary after dissection to grab with forceps for transferring the ovaries. Further, for smaller ovaries, transferring them with a pipette tip cut wide enough for the ovaries to easily fit within the tip avoids damage. If minor tissue damage results in a part of the ovary missing, it can be mitigated by a computational method where total oocyte numbers in the damaged sample can be extrapolated using intact samples of the same type (**Figure 6**).

However, computational simulations revealed that the accuracy of prediction diminishes with increasing size of the damaged area (100.8% ± 0.2, 97.2% ± 1.5, and 90.3% ± 1 for 10, 20, and 30% damage, respectively **Figure 6C**). Based on simulations, we recommend that samples with >30% loss be excluded from analysis. Multiple intact ovaries from the same sample type were used to calculate the average number of oocytes in the area similar to the one missing in damaged sample. This number was then used to predict the total number of oocytes in the ovary with damage. Using similar size area in the same ovary abutting the missing region may be used as an alternative but was not tested.

Another issue is to avoid contaminating cells that might cause autofluorescence. For pubertal ovaries, perfusion, as described above, with both 1x PBS and 1% PFA must be performed to eliminate blood cells that will cause autofluorescence (**Figure 2C**). Perfusion with PBS should continue until organs, especially the ovaries and kidneys, are cleared of blood and become white before switching to 1% PFA (**Figure 1E,F**). Inefficient perfusion with PBS will result in a high background that may mask and make the visualization of small oocytes difficult. Perfusion with

lower (1%) or higher (4%) percentages of PFA results in better image quality than perfusion with PBS alone; hence, the lower percentage of PFA was used.

Optimization of antibody staining requires attention to several variables. For the permeabilization step, 4 h was found to be ideal for this assay, with periods longer than 4 h (6–8 h tested) resulting in no staining at all. Because the amount and cost of antibodies used for large-scale immunostaining experiments can be high, this protocol was tested and optimized for reusing antibody mixes without any loss of immunostaining quality. For reuse, the antibody mixture must be supplemented with fresh antibody as described in the protocol. Washing steps are also critical for the quality of immunostaining and should be performed longer to achieve a better signal-to-noise ratio during imaging and should be determined for each antibody of choice. For best results, we recommend preparing the ScaleS4(0) clearing solution freshly for each use, while ScaleCUBIC-1 and ScaleCUBIC-2 can be stored at room temperature in the dark for ~1–2 months.

The ScaleCUBIC-1 clearing is performed at 37 °C; importantly, higher temperatures should be avoided as they will result in reagent precipitation, which can affect the quality of the immunostaining. Mounting multiple samples for imaging can be time-consuming. Agar or other embedding methods used in other protocols are labor-intensive and may need an additional re-clearing of samples[47,49,50]. Reusable silicon gaskets can be used as adhesive wells that are easy to use with coverslips and are offered in different sizes and depths to accommodate other sample sizes. To achieve high-quality images, a sufficient volume of clearing solution must be used; too little will result in poor image quality, and too much solution can leak onto the microscope. This step should be optimized for specific samples depending on their sizes. Glass-bottom dishes may be used but samples must be immobilized for imaging as even the slightest movements will distort the image. Silicon gaskets may be used in combination with a glass-bottom dish and top coverslip to immobilize the samples for imaging. However, this will limit the ability to flip the sample if imaging from both sides is needed due to the size of ovary.

Another critical choice for this large-scale, high-throughput approach was imaging on the Leica DIVE/4TUNE/FALCON platform with two tunable Spectra-Physics multiphoton (MP) lasers. The benefits of using the DIVE platform include ease of sample mounting (described above), minimization of optical distortion (compared to confocal platforms), and most importantly, imaging speed and management of acquired image data. Imaging samples with the multiphoton lasers at higher magnification (16x) is much faster and causes less photodamage than the confocal lasers on the Leica DIVE or SP8 using similar settings for image acquisition with LAS X software. The MP beam is low, its fluorophore excitation is highly localized to the focal point and achieves more depth at low magnification without inflicting photodamage despite a higher number of spatial/axial imaging steps (confocal: ~300–400 sections maximally, MP: >800 sections).

The 16x/NA0.6 objective allows correction for slight refractive index mismatches due to sample and mountant distribution along the optical axis via a mechanical correction collar, which is set optimally for maximal signal, half-way into the sample. Moreover, spherical structures, such as

oocytes, can be distorted by confocal image acquisition as depth-dependent localization of the confocal plane (signal) due to mountant and sample refractive index mismatches at a given pinhole setting can occur (**Figure 2D**). As the fluorescence signal is being captured via the instrument's internal pinhole to remove out-of-focus signal, the intrinsic optical distortion (spherical aberration) may get worse deeper into the sample, which is problematic for larger ovaries (i.e., ~400–600 micrometer thickness).

With the same matching lens-correction settings, virtually no spherical aberration can be detected on the DIVE MP system with varying emission wavelengths, thus simplifying quantification and co-localization studies (**Figure 2D**). Last, the high-power pulsed laser allows for exciting lower fluorophore concentration deep inside the sample, in particular, when it is used with the Z-depth excitation correction. Moreover, the capture of weaker signals is also enhanced by the MP hybrid detector (HyD-RLDs), which is a combination of regular photomultiplier tubes and avalanche photon-counting detectors, allowing for more than 30 times higher signal detection over a wide range of emission wavelengths.

Light sheet (LS) multiphoton microscopy is another emerging platform for 3D tissue imaging[47]. However, LS demands more setup time for macroscopic samples, including agar embedding and set up for imaging. Moreover, images acquired at higher magnification with sample rotation can generate large >100 GB files, which may be necessary to remove light sheet shadowing artifacts (due to refractive index mismatches of the outside medium and the interior of the sample, or sample-surface distortions). The presented method of mounting samples in solution in adhesive wells is simple and fast.

Moreover, this approach allows the imaging of multiple ovaries in one well with one setup and without flipping or rotation. However, flipping the coverslip "sandwich" may be needed for larger ovaries. The DIVE system imaging is faster than confocal and LS; at 16x magnification, the prepubertal ovary is imaged in 3–5 min (Z-step 2 µm) and the pubertal ovary in 1 h (Z-step 5 µm). Moreover, files generated in LAS X are of manageable size (2–20 GB), which is also critical for a large number of samples for downstream analysis. Although this immunostaining protocol was optimized for use in combination with the DIVE platform, immunostained samples can be imaged using other MP/LS platforms with some modifications.

The advantage of the whole ovary staining with 3D modeling protocol is the efficient and relatively easy data analysis compared to manual data acquisition in 2D analysis. The IMARIS 3D visualization and analysis software was chosen because it is commercially available and offered by many microscopy cores, does not require programming skills, and is compatible with many image acquisition software platforms such as LAS X from Leica or ZEN from ZEISS. With IMARIS, the standard parameters are set up as highlighted in the protocol section, and these parameters can be used for other images and samples with minor changes, thus improving reproducibility and efficiency.

Image analysis and quantification are optimized for IMARIS software; however, similar analyses can be done on other commercial or open-source data visualization software following similar

principles. In conclusion, an optimized protocol has been presented here for imaging entire ovaries for quantitative and qualitative analyses. This was purposefully adapted for the demands of the high-throughput processing that will be increasingly required for toxicology testing, clinical and diagnostic purposes, and genome-wide analyses of regulators of ovarian sufficiency and function.

ACKNOWLEDGMENTS

This work was supported by the National Institutes of Health grants (R01 HD093778 to E.B-F and T32 HD007065 to R.B). We thank Zachary Boucher for his assistance with radiation experiment. We thank Mary Ann Handel for critical reading of the manuscript. We gratefully acknowledge the contribution of Sonia Erattupuzha and the Microscopy Core Service at The Jackson Laboratory for expert assistance with the microscopy work described in this publication and Jarek Trapszo from the Scientific Instrument Services at The Jackson Laboratory for designing the 3D-printed adaptor slide.

DISCLOSURES

The authors have no conflicts of interest to disclose.

REFERENCES:

1. Pelosi, E., Forabosco, A., Schlessinger, D. Genetics of the ovarian reserve. *Frontiers in Genetics*. **6**, 308 (2015).
2. Pepling, M. E. From primordial germ cell to primordial follicle: mammalian female germ cell development. *Genesis*. **44** (12), 622–632 (2006).
3. Wilkosz, P., Greggains, G. D., Tanbo, T. G., Fedorcsak, P. Female reproductive decline is determined by remaining ovarian reserve and age. *PLoS One*. **9** (10), e108343 (2014).
4. Richardson, M. C., Guo, M., Fauser, B. C. J. M., Macklon, N. S. Environmental and developmental origins of ovarian reserve. *Human Reproduction Update*. **20** (3), 353–369 (2014).
5. Spears, N. et al. Ovarian damage from chemotherapy and current approaches to its protection. *Human Reproduction Update*. **25** (6), 673–693 (2019).
6. Morgan, S., Anderson, R. A., Gourley, C., Wallace, W. H., Spears, N. How do chemotherapeutic agents damage the ovary? *Human Reproduction Update*. **18** (5), 525–535 (2012).
7. Wesevich, V., Kellen, A. N., Pal, L. Recent advances in understanding primary ovarian insufficiency. *F1000Research*. **9**, doi: 10.12688/f1000research.26423.1 (2020).
8. Biswas, L. et al. Meiosis interrupted: the genetics of female infertility via meiotic failure. *Reproduction*. **161** (2), R13–R35 (2021).
9. Tam, P. P., Snow, M. H. Proliferation and migration of primordial germ cells during compensatory growth in mouse embryos. *Journal of Embryology and Experimental Morphology*. **64**, 133–147 (1981).
10. Pepling, M. E., Spradling, A. C. Female mouse germ cells form synchronously dividing cysts. *Development*. **125** (17), 3323–3328 (1998).

11. Pepling, M. E., Spradling, A. C. Mouse ovarian germ cell cysts undergo programmed breakdown to form primordial follicles. *Developmental Biology*. **234** (2), 339–351 (2001).
12. Adams, I. R., McLaren, A. Sexually dimorphic development of mouse primordial germ cells: switching from oogenesis to spermatogenesis. *Development*. **129** (5), 1155–1164 (2002).
13. McLaren, A., Southee, D. Entry of mouse embryonic germ cells into meiosis. *Developmental Biology*. **187** (1), 107–113 (1997).
14. Findlay, J. K., Hutt, K. J., Hickey, M., Anderson, R. A. How is the number of primordial follicles in the ovarian reserve established? *Biology of Reproduction*. **93** (5), 111 (2015).
15. Tilly, J.L. Commuting the death sentence: how oocytes strive to survive. *Nature Reviews. Molecular Cell Biology*. **2** (11), 838–848 (2001).
16. Baker, T. G. A quantitative and cytological study of germ cells in human ovaries. *Proceedings of the Royal Society of London. Series B, Biological Sciences*. **158**, 417–433 (1963).
17. Baker, T. G. A quantitative and cytological study of oogenesis in the rhesus monkey. *Journal of Anatomy*. **100** (Pt 4), 761–776 (1966).
18. Kurilo, L. F. Oogenesis in antenatal development in man. *Human Genetics*. **57** (1), 86–92 (1981).
19. Matova, N., Cooley, L. Comparative aspects of animal oogenesis. *Developmental Biology*. **231** (2), 291–320 (2001).
20. Malki, S., van der Heijden, G. W., O'Donnell, K. A., Martin, S. L., Bortvin, A. A role for retrotransposon LINE-1 in fetal oocyte attrition in mice. *Developmental Cell*. **29** (5), 521–533 (2014).
21. Tharp, M. E., Malki, S., Bortvin, A. Maximizing the ovarian reserve in mice by evading LINE-1 genotoxicity. *Nature Communications*. **11** (1), 330 (2020).
22. Rinaldi, V. D., Bolcun-Filas, E., Kogo, H., Kurahashi, H., Schimenti, J. C. The DNA damage checkpoint eliminates mouse oocytes with chromosome synapsis failure. *Molecular Cell*. **67** (6), 1026–1036.e2 (2017).
23. Bolcun-Filas, E., Rinaldi, V. D., White, M. E., Schimenti, J. C. Reversal of female infertility by *Chk2* ablation reveals the oocyte DNA damage checkpoint pathway. *Science*. **343** (6170), 533–536 (2014).
24. Pepling, M. E. Follicular assembly: mechanisms of action. *Reproduction*. **143** (2), 139–149 (2012).
25. Tingen, C., Kim, A., Woodruff, T. K. The primordial pool of follicles and nest breakdown in mammalian ovaries. *Molecular Human Reproduction*. **15** (12), 795–803 (2009).
26. Wallace, W. H. B., Kelsey, T. W. Human ovarian reserve from conception to the menopause. *PLoS One*. **5** (1), e8772 (2010).
27. Pepling, M. E. et al. Differences in oocyte development and estradiol sensitivity among mouse strains. *Reproduction*. **139** (2), 349–357 (2010).
28. Nelson, S. M., Anderson, R. A. Prediction of premature ovarian insufficiency: foolish fallacy or feasible foresight? *Climacteric*. 1–10, doi: 10.1080/13697137.2020.1868426 (2021).
29. Wood, M. A., Rajkovic, A. Genomic markers of ovarian reserve. *Seminars in Reproductive Medicine*. **31** (6), 399–415 (2013).
30. Tilly, J. L. Ovarian follicle counts--not as simple as 1, 2, 3. *Reproductive Biology and Endocrinology*. **1**, 11 (2003).

31. Winship, A. L., Sarma, U. C., Alesi, L. R., Hutt, K. J. Accurate follicle enumeration in adult mouse ovaries. *Journal of Visualized Experiments: JoVE*. (164), doi: 10.3791/61782 (2020).
32. Fiorentino, G., Parrilli, A., Garagna, S., Zuccotti, M. Three-dimensional imaging and reconstruction of the whole ovary and testis: a new frontier for the reproductive scientist. *Molecular Human Reproduction*. **27** (3), gaab007 (2021).
33. Sarma, U. C., Winship, A. L., Hutt, K. J. Comparison of methods for quantifying primordial follicles in the mouse ovary. *Journal of Ovarian Research*. **13** (1), 121 (2020).
34. Skodras, A., Marcelli, G. Computer-generated ovaries to assist follicle counting experiments. *PLoS One*. **10** (3), e0120242 (2015).
35. Sonigo, C. et al. High-throughput ovarian follicle counting by an innovative deep learning approach. *Scientific Reports*. **8** (1), 13499 (2018).
36. Myers, M., Britt, K. L., Wreford, N. G. M., Ebling, F. J. P., Kerr, J. B. Methods for quantifying follicular numbers within the mouse ovary. *Reproduction*. **127** (5), 569–580 (2004).
37. Kagami, K., Shinmyo, Y., Ono, M., Kawasaki, H., Fujiwara, H. Three-dimensional evaluation of murine ovarian follicles using a modified CUBIC tissue clearing method. *Reproductive Biology and Endocrinology*. **16** (1), 72 (2018).
38. Rinaldi, V. D., Hsieh, K., Munroe, R., Bolcun-Filas, E., Schimenti, J. C. Pharmacological inhibition of the DNA damage checkpoint prevents radiation-induced oocyte death. *Genetics*. **206** (4), 1823–1828 (2017).
39. Malki, S., Tharp, M. E., Bortvin, A. A whole-mount approach for accurate quantitative and spatial assessment of fetal oocyte dynamics in mice. *Biology of Reproduction*. **93** (5), 113 (2015).
40. Susaki, E. A. et al. Whole-brain imaging with single-cell resolution using chemical cocktails and computational analysis. *Cell*. **157** (3), 726–739 (2014).
41. Hama, H. et al. ScaleS: an optical clearing palette for biological imaging. *Nature Neuroscience*. **18** (10), 1518–1529 (2015).
42. Gage, G. J., Kipke, D. R., Shain, W. Whole animal perfusion fixation for rodents. *Journal of Visualized Experiments: JoVE*. (65), 3564 (2012).
43. Capel Lab at Duke University Medical Center. Microscope slide (25x75) with inset for coverslips (22x22). NIH 3D Print Exchange. https://3dprint.nih.gov/discover/3DPX-009765 (2018)
44. Niu, W., Spradling, A. C. Two distinct pathways of pregranulosa cell differentiation support follicle formation in the mouse ovary. *Proceedings of the National Academy of Sciences of the United States of America*. **117** (33), 20015–20026 (2020).
45. Livera, G., Petre-Lazar, B., Guerquin, M. -J., Trautmann, E., Coffigny, H., Habert, R. p63 null mutation protects mouse oocytes from radio-induced apoptosis. *Reproduction*. **135** (1), 3–12 (2008).
46. Carroll, J., Marangos, P. The DNA damage response in mammalian oocytes. *Frontiers in genetics*. **4**, 117 (2013).
47. McKey, J., Cameron, L. A., Lewis, D., Batchvarov, I. S., Capel, B. Combined iDISCO and CUBIC tissue clearing and lightsheet microscopy for in toto analysis of the adult mouse ovary†. *Biology of Reproduction*. **102** (5), 1080–1089 (2020).
48. McKey, J., Anbarci, D.N., Bunce, C., Capel, B. Integration of mouse ovary morphogenesis with developmental dynamics of the oviduct, ovarian ligaments, and rete ovarii. *bioRxiv*. doi: 10.1101/2021.05.21.445181 (2021).

49. Udan, R. S., Piazza, V. G., Hsu, C. -W., Hadjantonakis, A. -K., Dickinson, M. E. Quantitative imaging of cell dynamics in mouse embryos using light-sheet microscopy. *Development*. **141** (22), 4406–4414 (2014).
50. Di Giovanna, A. P. et al. Tailored sample mounting for light-sheet fluorescence Microscopy of clarified specimens by polydimethylsiloxane casting. *Frontiers in Neuroanatomy*. **13**, 35 (2019).

Figure1

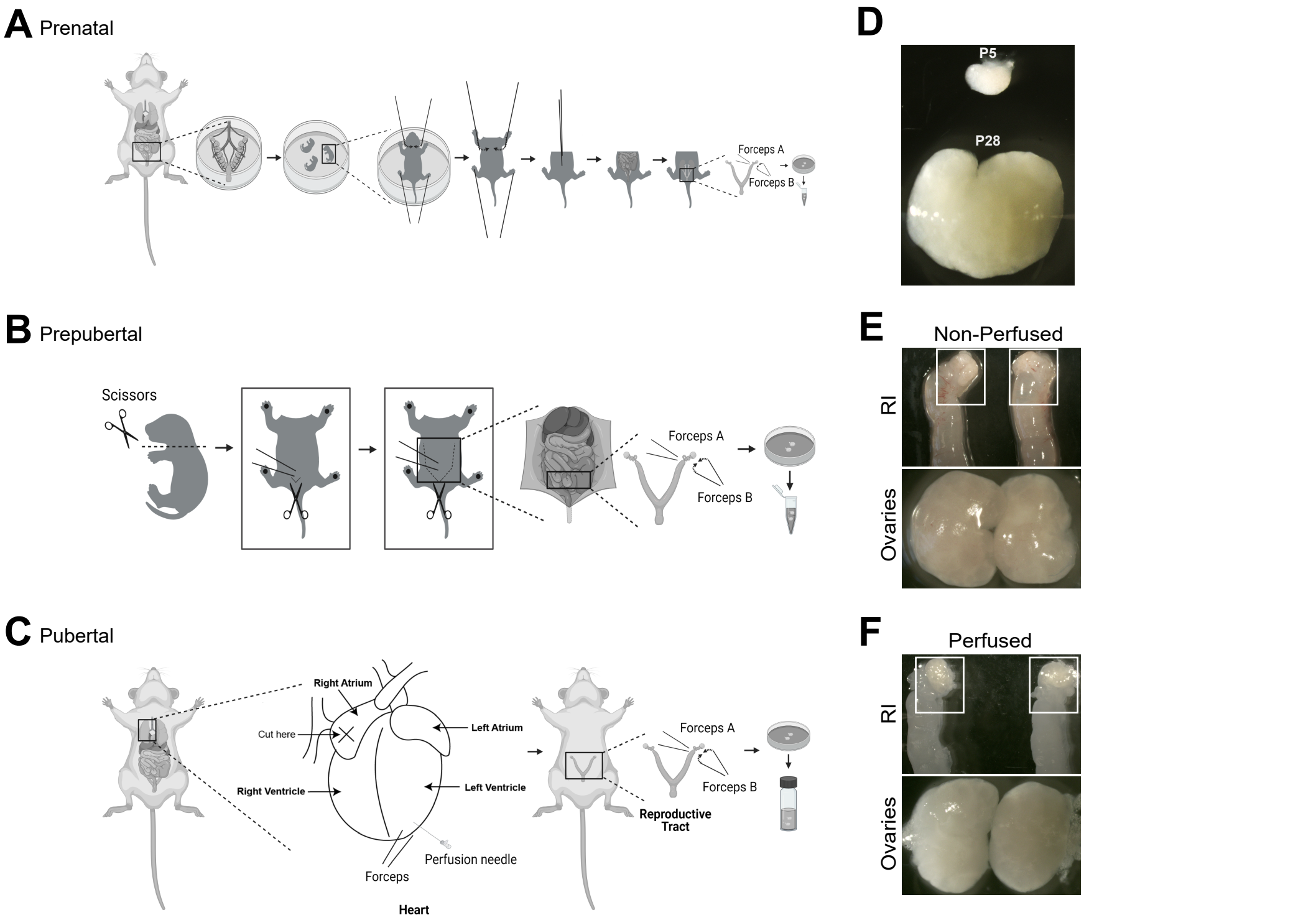

Figure2

Click here to access/download;Figure;Boateng Figure 2.pdf

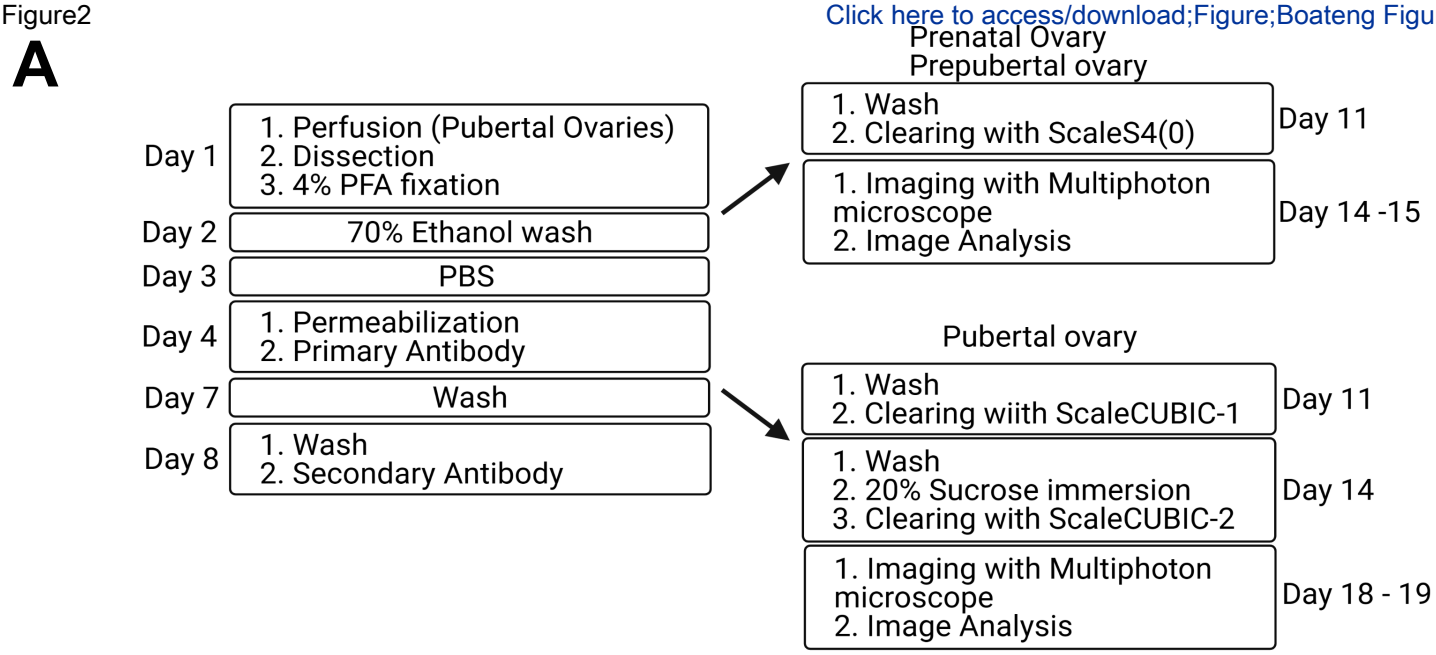

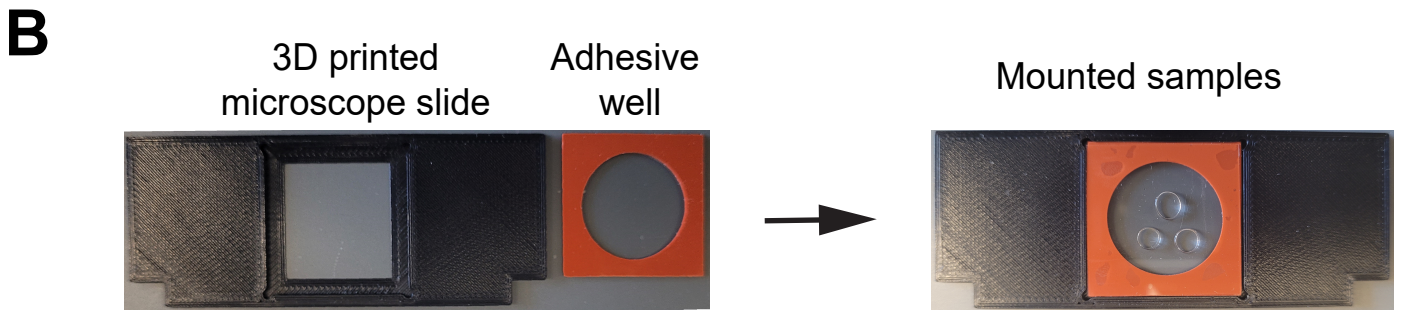

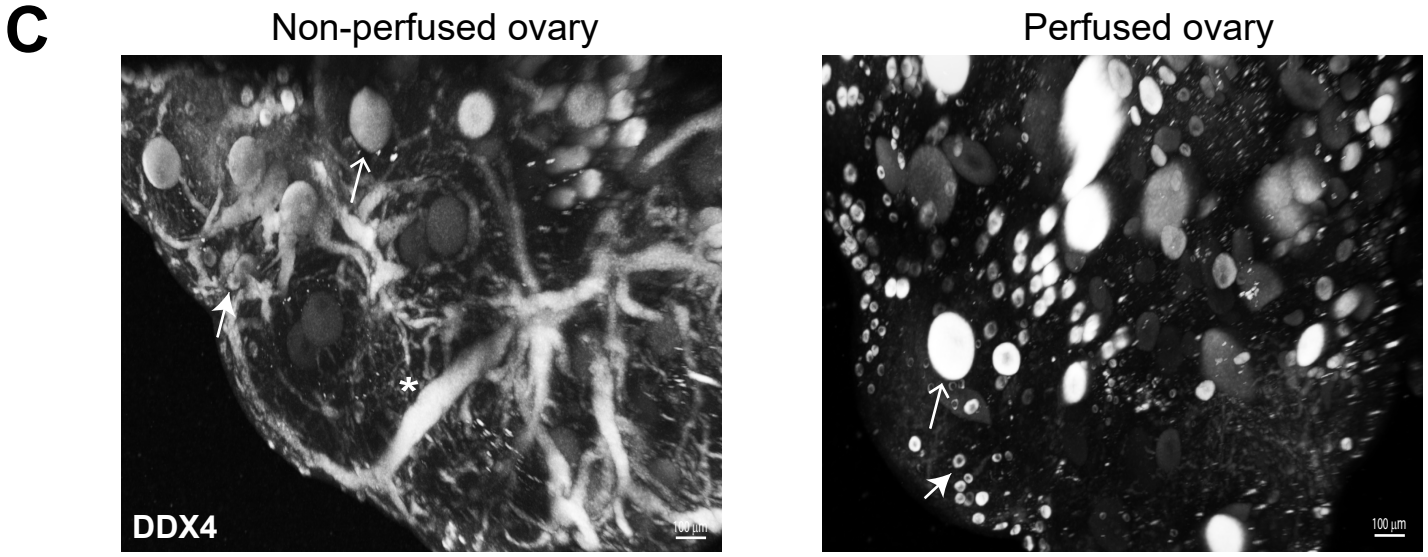

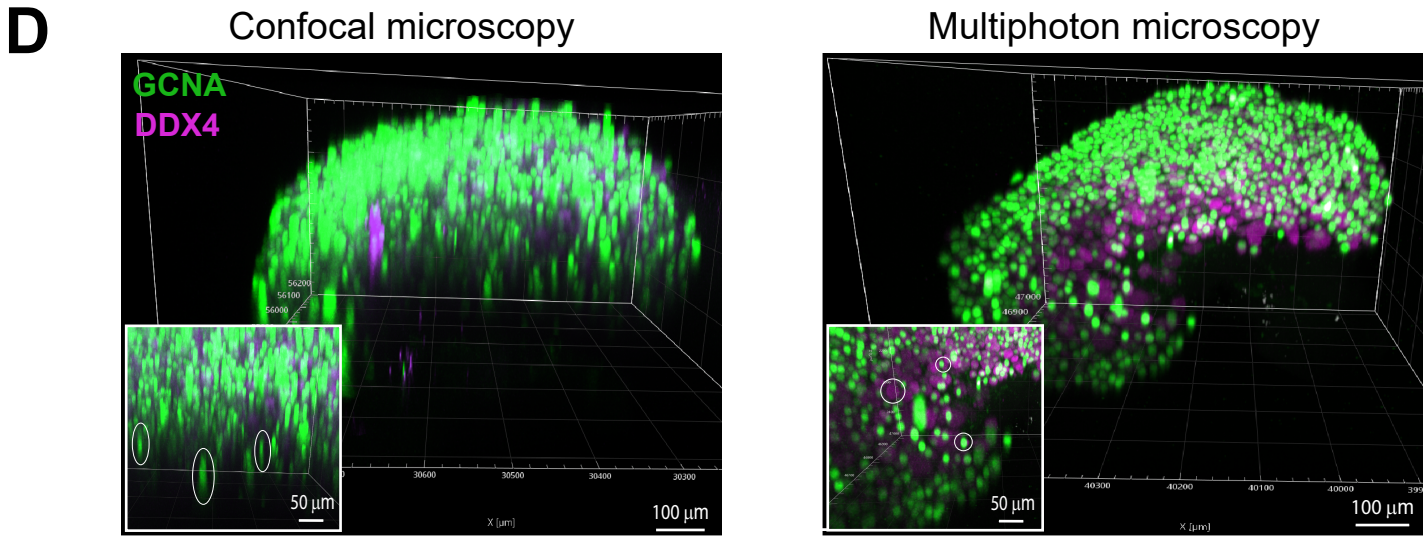

Figure3

Click here to access/download;Figure;Boateng Figure 3.pdf

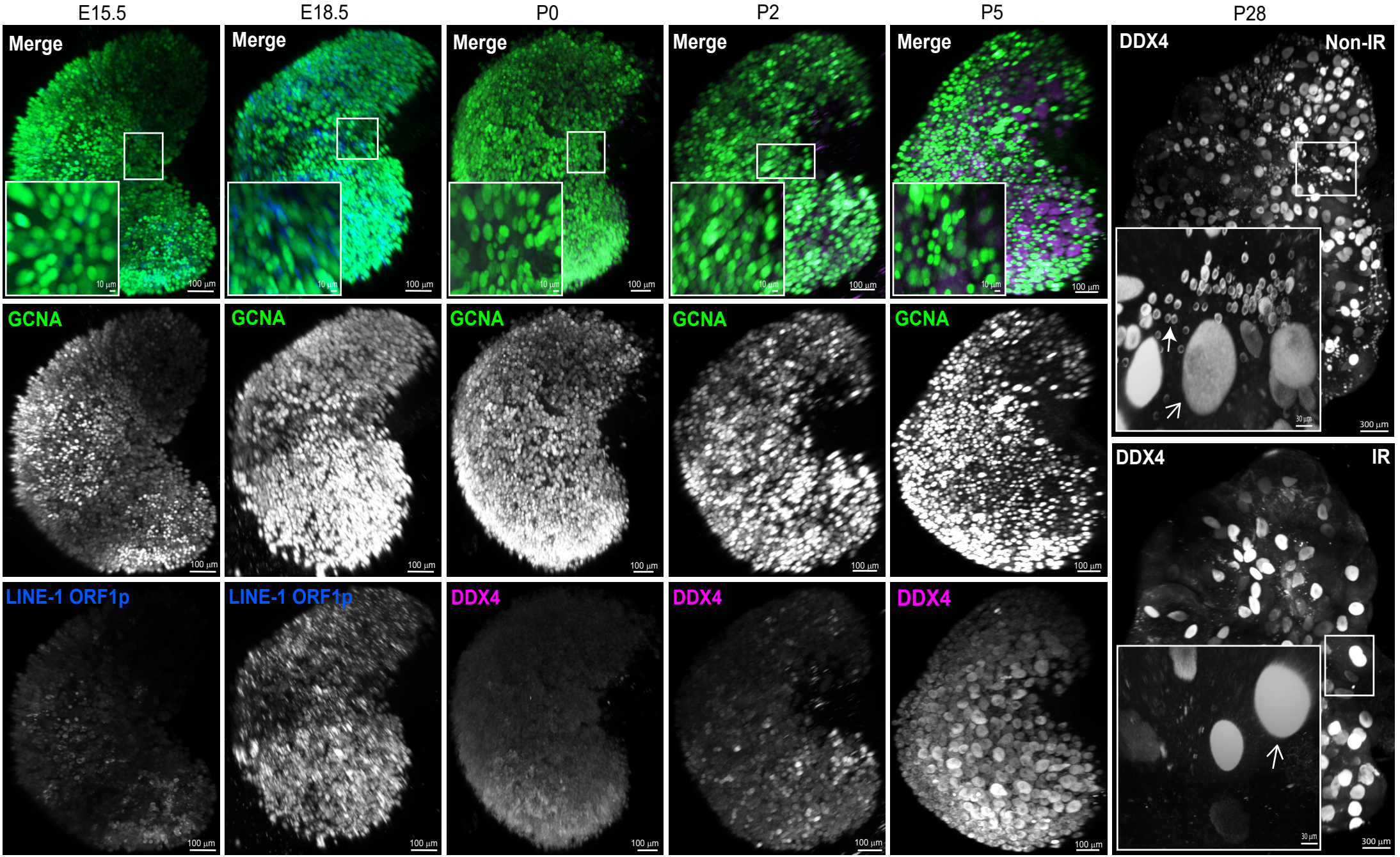

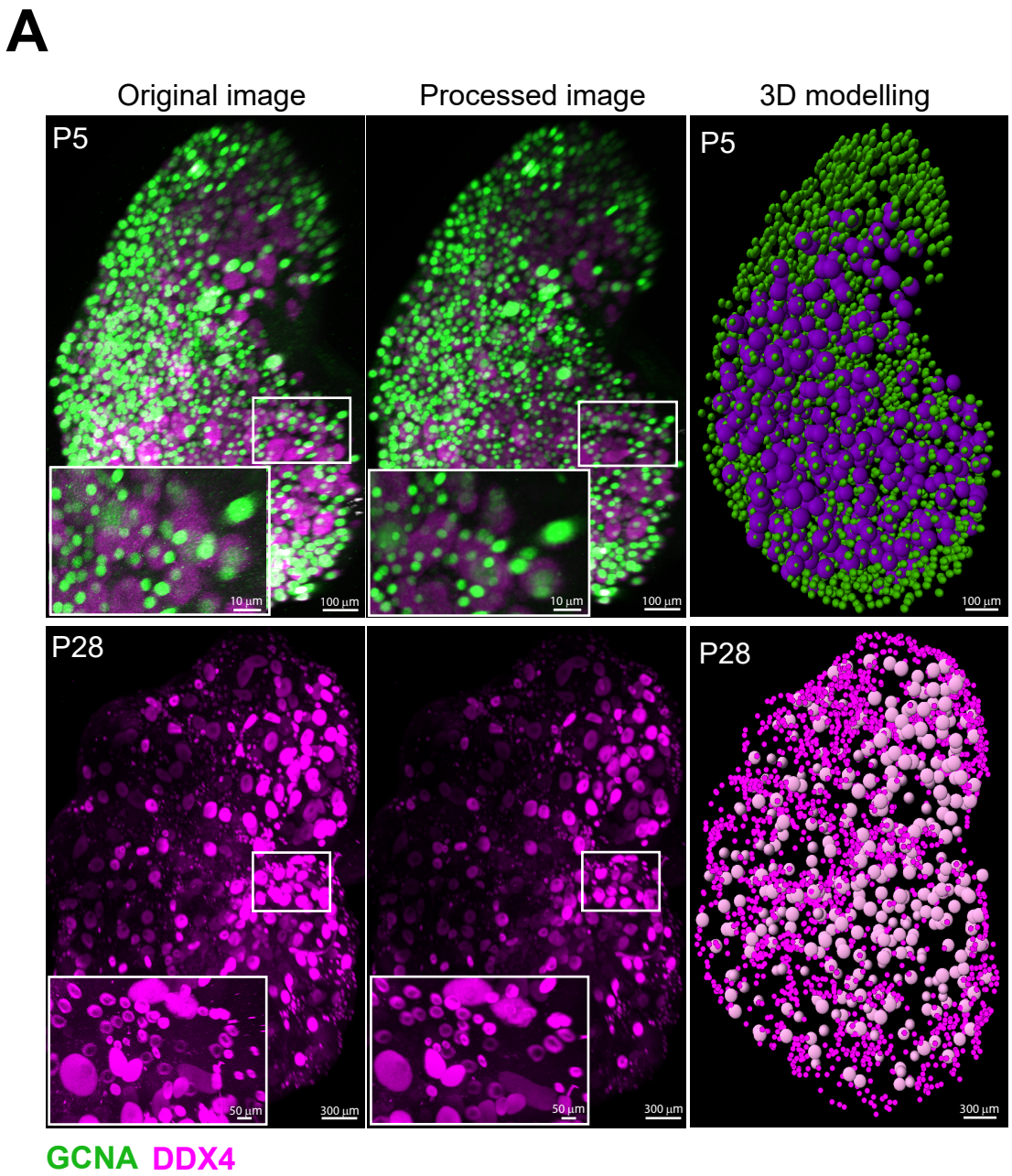

Figure5

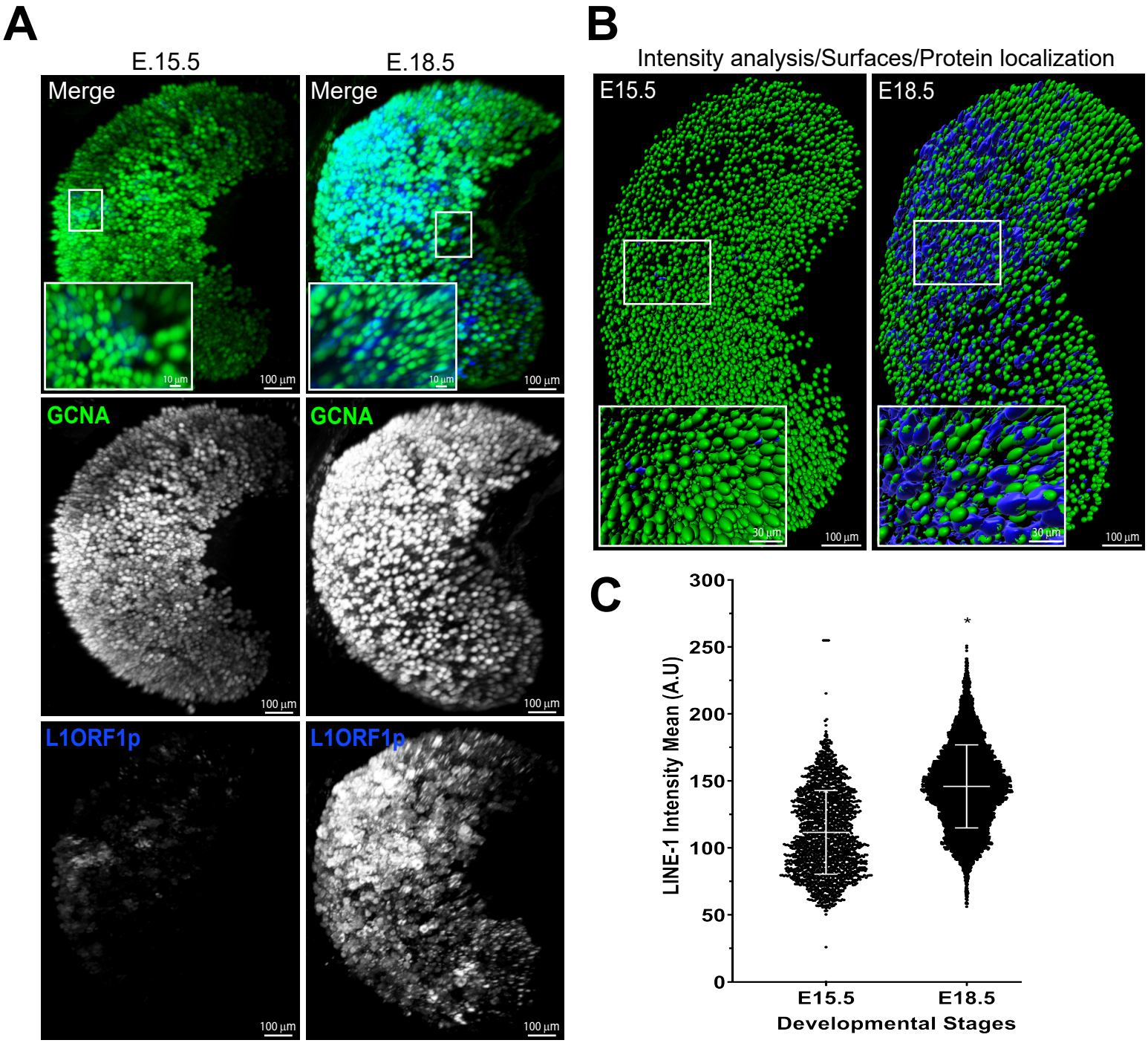

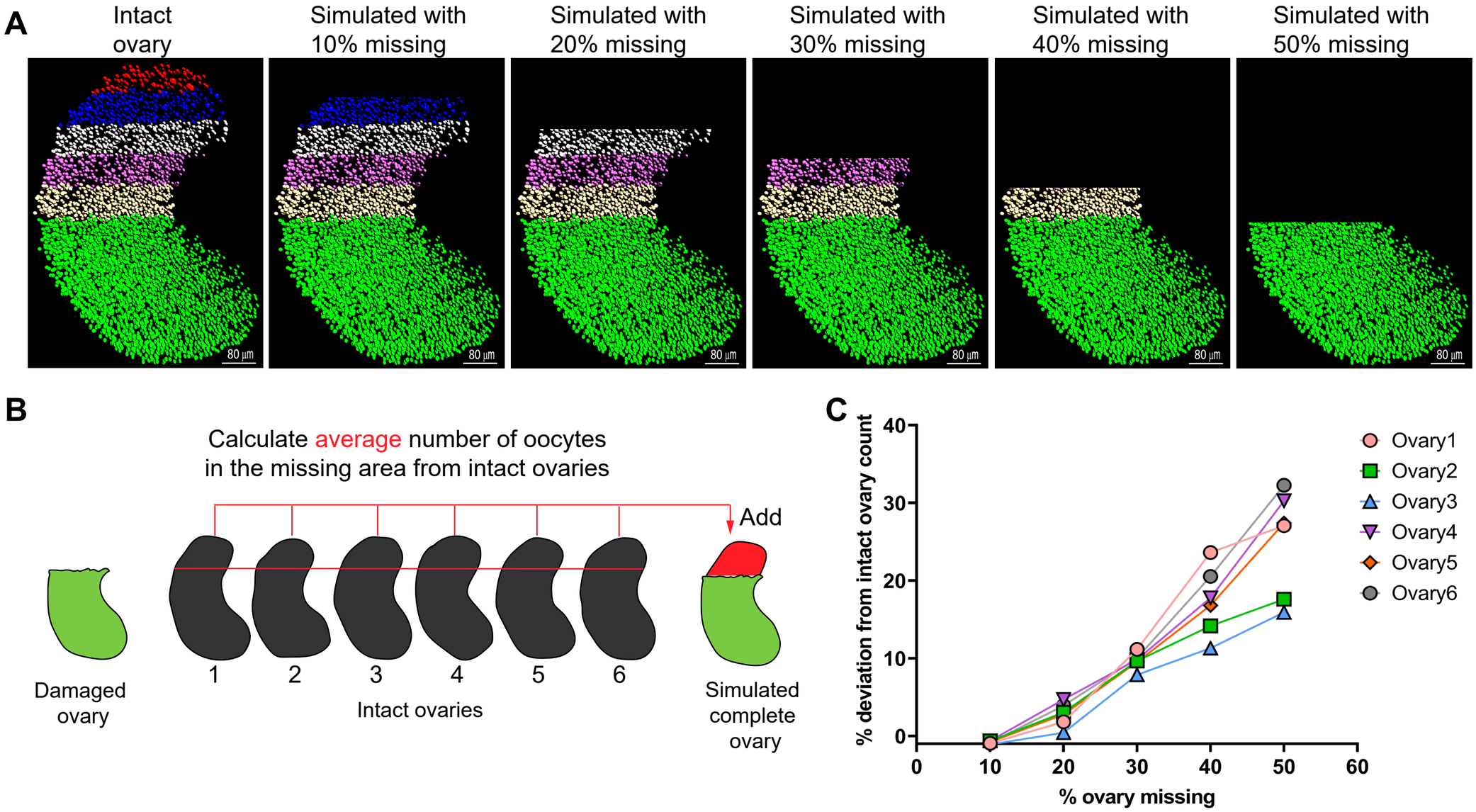

Click here to access/download
Video or Animated Figure
JOVE Movie1.mp4

Table 1

Solutions and buffers	Reagent(s)	Composition
Fixative	Paraformaldehyde	4% (v/v)
Permeabilization buffer	Polyvinyl alcohol (PVA)	0.2% (w/v)
	Sodium borohydride	0.1% (w/v)
	Triton X-100	1.5% (v/v)
Blocking buffer	Bovine Serum Albumin (BSA)	3% (w/v)
	1 M Glycine	2% (w/v)
	Triton X-100	0.1% (v/v)
	200x Penicillin-Streptomycin	1% (v/v)
	10% Sodium azide	0.2% (v/v)
	goat serum	10% (v/v)
Washing buffer	PVA	0.2% (w/v)
	Triton X-100	0.15% (v/v)
	10% Sodium azide	0.1% (v/v)
ScaleS4(0) solution (pH 8.1)	D-Sorbitol	40% (w/v)
	Urea	24% (w/v)
	Glycerol	10% (v/v)
	DMSO	20% (v/v)
ScaleCUBIC-1 solution	Urea	25% (w/v)
	N,N,N′,N′-Tetrakis(2-Hydroxypropyl)ethylenediamine	25% (v/v)
	Triton X-100	15% (v/v)
Sucrose Solution	Sucrose	20%(w/v)
ScaleCUBIC-2 solution	Sucrose	50% (w/v)
	Urea	25% (w/v)
	Triethanolamine	10% (w/v)
	Triton X-100	0.1% (v/v)

Reviewers' comments:

We thank the reviewers for their thoughtful comments. Below we have highlighted changes made to improve the manuscript.

Reviewer #1:
Major Concerns:
The method requires intact ovaries after fine dissections and more than two weeks of processing for immunofluorescence that can introduce damage to the tissue as discussed in lines 726-731. I am concerned that this method may not be easily carried out by those who are not skilled at dissection and potentially waste ovaries that could have been used unless there is a way to address minor damage computationally. Include a way to judge whether an ovary is too damaged to process during image analysis, or in the case of minor damage, how to estimate the number of oocytes in a damaged region computationally. For example, quantify the number of oocytes in another similar region of the ovary that is intact and extrapolate this number to the damaged region area when reasonable.

We thank the reviewer for this idea. We have now included a method and simulations showing that computational correction for small damage may be done using data from intact ovaries. (Protocol 7.19-7.23) ;Figure 6, L694-700; 784-793)

Minor Concerns:
1. Title - The emphasis on 3D visualization and multiphoton microscopy in the title does not fully reflect the protocol that also demonstrates the acquisition, immunofluorescence staining, and clearing of ovarian tissue.

We have change the title to better reflect the content of this protocol. New title "Whole Ovary Immunofluorescence, Clearing and Imaging by Multiphoton Microscopy for Quantitative 3D Analysis of the Developing Ovarian Reserve in Mouse.

2. Applications - Analysis of male germ cell development, development of the somatic cells of the ovary, and human ovarian tissues are potential applications worth discussing.

We agree with the reviewer that this protocol will be feasible for other applications. We have indeed used it for fetal male gonads. The protocol would need to be optimized for postnatal testes but we have not done it. We have included this in the discussion. We have no experience in immunostaining human ovarian tissue therefore we will refrain from making any recommendations. Theoretically this protocol should work for fragments of human ovary. However, perfusion is not an option for human ovaries therefore it may be difficult to extrapolate the protocol from much smaller mouse ovaries.

3. Imaging - For the acquisition of multiple colors, imaging the entire Z stack in the color of the longest wavelength first to avoid photobleaching is important.

The advantage of multiphoton imaging is that one laser is used to capture images for two wavelengths (555 and 647) at the same time. Additionally, the 2-photon laser acquisition yields low background and hardly any photobleaching throughout a long Z-stack acquisition. This is explained under in discussion lines 830-836.

4. Sample setup - In sample setup for microscopy, include the exact sizes and depths for reusable silicon gaskets for corresponding stages of ovaries. A glass-bottom dish may be a simple alternative suggestion for mounting ovaries.

We have included details of sizes and depths of the reusable silicon gaskets in the table of reagents and also under the image set up section 6.1. We have tested a glass-bottom dish and concluded that our set up is more efficient. We found that samples placed in a glass-bottom dish move around during imaging, thereby distorting the image. We tried to construct a "well" inside a glass-bottom dish to restrict sample movement which improved imaging but was not easier. It required use of expensive dishes and eliminated the option to flip the sample to image from the other side. Base on the time we spent on optimizing this method without success we do not recommend this method. Instead we offer a more reliable and relatively cheap method using reusable silicon gasket. 3D printing becomes more available in research institutions and there are 3D-printing hubs that researcher can use to print inserts if they have no access.

5. Table of materials/equipment - Multiphoton microscope and IMARIS software version used are missing.

We have update the table with details about microscope and software version. (Supplementary)

6. Typographical comments - In line 56, "and now termed oocytes" is underlined. In line 373, "7. Imaging" is not the same font/color as the previous steps. Indentation is not consistent throughout the protocol.

We corrected typographical errors in revised manuscript.

Reviewer #2:
Concerns:
However a context of the follicular developmental stage would be useful.

We regret but we are unable to address reviewer's comment. Due to the absence of granulosa cell markers in our protocol it is not possible to differentiate follicular stages.

Reviewer #3:
Minor Concerns:
The authors describe and provide a cartoon (Figure 1) of the dissection of embryonic ovaries and prepubertal and pubertal ovaries; however, a video of the dissection procedures would be helpful for those who have not performed these dissections previously.

Video including the dissection and other part's of the protocol will be produced to accompany this publication. We will keep in mind reviewer's comment when we film the procedure.

The authors provide detailed protocols for counting oocytes/follicles and for quantifying immunofluorescence intensity using the Leica/DIVE/4TUNE/FALCON with two multiphoton lasers

coupled with Imaris software. These protocols are less generalizable than the dissection and immunostaining protocols because they will vary with the microscopy platform that is available to the user. The immunostaining and clearing protocols are standard and have been previously published.

We agree with the reviewer that not all researchers have access to the same equipment and software. When we started our project we were where many of our colleagues may be now; considering which imaging platform to use or which software to choose. We tried confocal and light sheet and found multiphoton to be superior for large scale imaging projects. We present this protocol for users as a recommendation. If they have a choice or consider new purchase this protocol may be helpful. Many imaging software require coding skills which may be limitation for biologists. We acknowledge that IMARIS or other commercial software may be expensive but commercial software may be provided by imaging facilities. Even though our protocol is for a specific platform and software many aspects of the protocol and analysis can be extended to other platforms with some optimization as mentioned throughout the manuscript.

Editorial comments:

1. Please take this opportunity to thoroughly proofread the manuscript to ensure that there are no spelling or grammar issues. Please define all abbreviations at first use.

- *Current version of the manuscript was proofread by a scientific writer.*

2. Please provide an email address for each author.

- *As it is not specified where to provide email addresses of all the authors after authorship.*

3. Being a video based journal, JoVE authors must be very specific when it comes to the humane treatment of animals. Regarding animal treatment in the protocol, please add the following information to the text:

a) What was the age and weight of the mice?

Prenatal and prepuberal were not weighed as there was no need to weight them. The pubertal weight varies from 13.09g- 14.86g and the weight was used to determine the amount of tribromoethanol needed for euthanasia

b) Please specify the euthanasia method without highlighting it.

- Described for pregnant mothers in point 1.1
- Described in point 1.4 for prenatal stages
- Described in point 2.1 for neonatal pups
- Described in point 3.1 for pubertal perfused mice. Injection with tribromoethanol is used for anesthesia prior to perfusion in 3.2.

c-g) Do not apply.

- Anesthesia was not used for survival surgery. We added information that perfusion is a terminal euthanasia procedure in point 3.1.

4. JoVE cannot publish manuscripts containing commercial language. This includes trademark symbols (™), registered symbols (®), and company names before an instrument or reagent. Please remove all commercial language from your manuscript and use generic terms instead. All commercial products should be sufficiently referenced in the Table of Materials and Reagents.
For example: in Eppendorf tubes; Leica DIVE/4TUNE/FALCON; LAS X 3.5.6 software; FastWells Reagent Barrier; X-Cite 120LED, Excelitas; LAS X navigator; with IMARIS 3D/4D image visualization and analysis software etc
Obviously, if you have optimized your protocol with certain instruments/reagents/software, you will need to mention them, but include just the bare minimum information (e.g., name of product) in the manuscript and come up with a generic term to refer to the product (include this in the comments column in the Table of Materials) after the first mention so that you don't keep repeating commercial terms throughout the paper. Please revise the text, especially in the protocol, to avoid the use of any personal pronouns (e.g., "we", "you", "our" etc.). You can mention products or software in the discussion if you wish to compare them to what you have used.

- *We revised our manuscript to limit the use of commercial language. We left the minimum we deemed necessary for clarity.*

5. Please ensure that all text in the protocol section is written in the imperative tense as if telling someone how to do the technique (e.g., "Do this," "Ensure that," etc.). The actions should be described in the imperative tense in complete sentences wherever possible. Avoid usage of phrases such as "could be," "should be," and "would be" throughout the Protocol. Any text that cannot be written in the imperative tense may be added as a "Note." However, notes should be concise and used sparingly. Please include all safety procedures and use of hoods, etc.

- *We have revised the manuscript to address this.*

6. Please note that your protocol will be used to generate the script for the video and must contain everything that you would like shown in the video. Please add more details to your protocol steps. Please ensure you answer the "how" question, i.e., how is the step performed? Alternatively, add references to published material specifying how to perform the protocol action. Please add more specific details (e.g., button clicks for software actions, numerical values for settings, etc) to your protocol steps. Especially the setting of parameters, gain etc. Consider providing supplemental material (tables, Word files) with all these settings. Including enough details will help to show representative results and also film your video. There should be enough detail in each step to supplement the actions seen in the video so that viewers can easily replicate the protocol.

- *We have revised the manuscript to address this and included Table S1 and Figure S1 with more details for image acquisition.*

7. Please format the manuscript as: paragraph Indentation: 0 for both left and right and special: none, Line spacings: single. Please include a single line space between each step, substep and note in the protocol section. Please use **Calibri 12 points and one-inch margins on all the side**. Please include a ONE LINE SPACE between each protocol step and then HIGHLIGHT up to 3 pages of protocol text for inclusion in the protocol section of the video.

- *We have revised the manuscript with correct formatting.*

8. Provide reaction set-ups and solution composition as Tables in separate .xls or .xlsx files uploaded to your Editorial Manager account. These tables can then be referenced in the protocol text.

- Not applicable

9. Please include a scale bar for all images taken with a microscope to provide context to the magnification used. Define the scale in the appropriate Figure Legend.

- All images have defined scale bars.

10. Please remove the embedded Table from the manuscript. All tables should be uploaded separately to your Editorial Manager account in the form of an .xls or .xlsx file. The table legend or caption (title and description) should appear in the Figure and Table Legends section after the Representative Results in the manuscript text.

- Table is now presented as separate file.

Supplemental Figure1

Click here to access/download;Supplemental File (Figures, Permissions, etc.);Boateng Figure S1.pdf

Acquisition Mode, XY, Z-Stack

Laser Settings

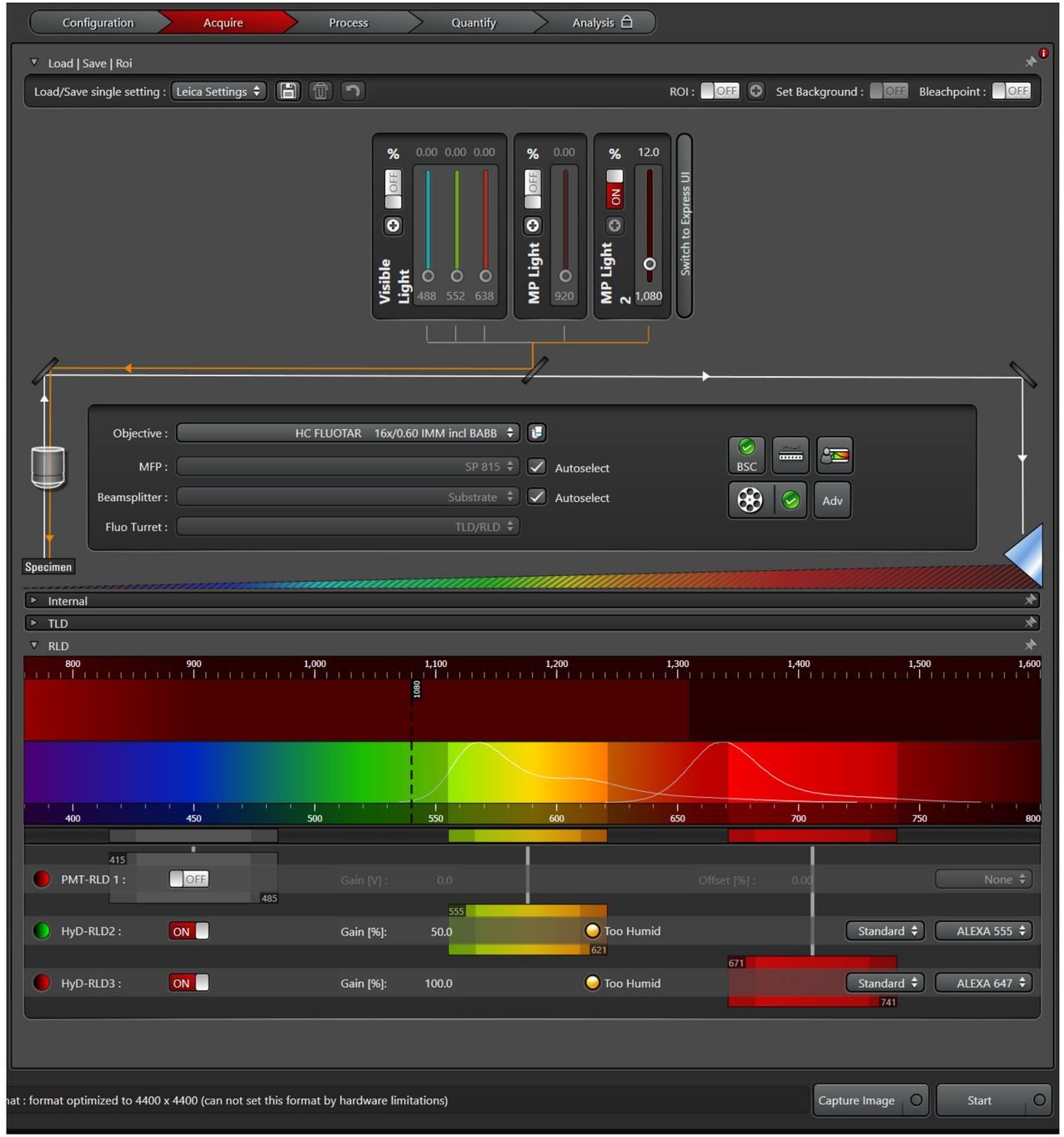

Linear Z-compensation

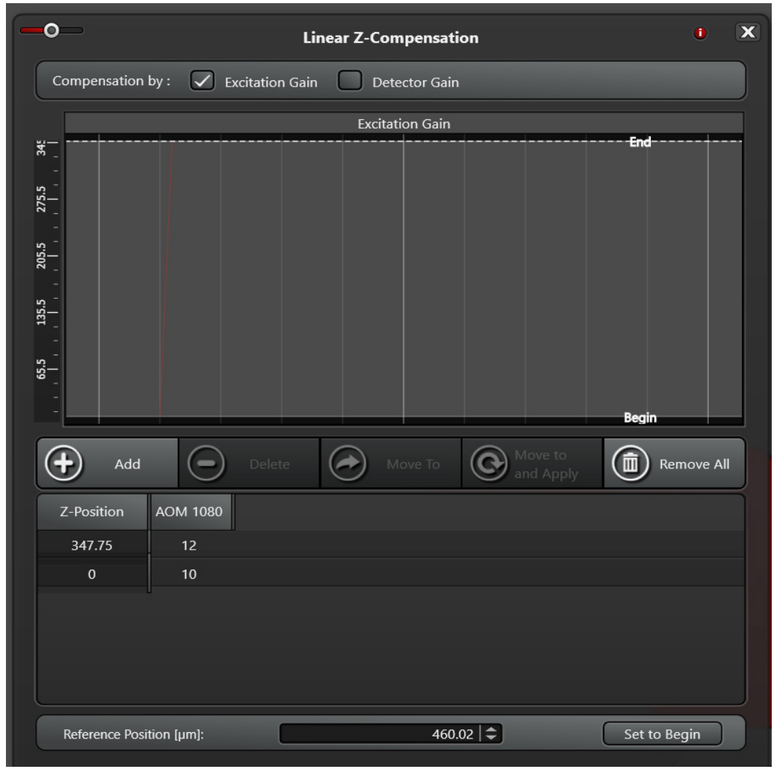

Supplemental Table S1

Click here to access/download;Supplemental File (Figures, Permissions, etc.);Supplemental Table S1_final.xls

Acquisition Settings
Scanning Format
Speed
Bidirectional X
Phase X
Line Average
Line Accu
Frame Average
Frame Accu
Z-Step Size
Linear Z-Compensation
555 Detector
667 Detector

Supplemental Table S1: Image acquisition settings

Description
Acquisition Mode, XY, Z-Stack
Pixels numbers of an image and thus its resolution
Scanning speed of lasers
Laser scan rows in the same direction
Value that compensates for offset between rows scanned
Defines how often the laser scans and acquires each line
Specify number of frames that will be created for each scan cycle
Specifies the offset between the images
Linear Z-compensation
Compensate for a decrease in brightness while acquiring a z-stack
Detector Settings
Detectors for image acquisition

Values	
1024 x 1024	
600	
Active	
Automatically determined after bidirectional activation	
1	
1	
1	
1	
2 (Prenatal and early postnatal ovaries) (Pubertal ovaries)	5
Excitation gain	
Gain used: 50 - 100	
Gain used: 100 - 200	